TO OPTIMIZE THE EXTRACTION OF OIL AND DIETARY FIBRE FROM SEEDS OF PASSION FRUIT AND STUDY THEIR EXTRACTION KINETICS AND PROPERTIES.

CHAPTER 5 (SECTION A & B)

CHAPTER 5 SECTION A

KINETIC MODELLING OF COMBINED ULTRASONICATION AND SOXHLET-BASED EXTRACTION OF OIL FROM PASSION FRUIT SEED AND ITS COMPARISON AND EVALUATION OF PHYSICOCHEMICAL PROPERTIES OF OPTIMIZED EXTRACTED OIL

5A.1. Introduction

A significant issue with passion fruit in the manufacturing sector is the waste generated from the discarded peels and seeds, which accounts for more than half of the fruit weight and is gaining the interest of researchers as the seed and peel contain high quantities of bioactive compounds [27]. Passion fruit seeds (PFS) make up between 8.24 and 16.18 % of the fruit weight [27]. The oil content in passion fruit seeds (PFSO) ranges from 22–30 % and is rich in polyphenols, phytosterols, essential fatty acids, and has a major proportion of unsaturated fatty acids [23,25,28]. Antimicrobial properties are displayed by passion fruit seed oil [13,14]. According to Ramiya et al. [25], the seed oil has a considerable antioxidant activity of 34 mg/mL (EC_{50} DPPH) and roughly 570 mg GAE/kg oil of total phenolic compounds.

Leaching, or solid-liquid extraction, has been widely utilised in the food processing and other sectors to extract the target compounds from plant food matrices by employing a proper solvent. Because seeds typically have low oil percentages, efforts must be made to increase yield while lowering overall process costs. Technology-wise, the extraction process is mostly influenced by the operating variables such as the solvent and extraction method used, the operating temperature, the solid to solvent ratio, and the extraction duration. By optimising these factors, the extraction yield may be increased [19,21]. Ethanol is the widely used solvent because it is less harmful and has no impurities [32].

High-energy extraction methods, which are based on the principles of green chemistry and bio-refinery techniques, have recently attracted a lot of attention, and have become a hot topic in the field of oil extraction due to their quick extraction rates, high extraction yields, minimal negative effects on the extracted compounds, improved extraction of thermosensitive nutritional components, and lower processing temperatures [6,11,21].

Over the past few years, several novel techniques for obtaining seed oils have been researched upon, including mechanical compression, ultrasonic extraction,

microwave extraction, and supercritical fluid extraction [15]. Edible vegetable oils are traditionally extracted via mechanical pressing and/or liquid solvent-based extraction techniques, notwithstanding their limitations. The main drawbacks of mechanical pressing include low extraction rates, air and light exposure, and shelf-life loss. Solvent-based conventional extractions typically involve a lengthy process that consumes a lot of energy, resulting in high solvent usage, high toxicity, and environmental risks and the loss of volatile compounds [22].

Supercritical extraction and ultrasonic assisted extraction (UAE) are some of the most promising alternative processes [22]. UAE has been used to extract oil from raspberries [32], sweet passion fruit seeds [28], Spanish flax seeds [9], and tara seeds [15]. However, it has some drawbacks, including the inability of the solvent to be refreshed during the process, which reduces its efficiency, the need for filtration and solvent evaporation in the subsequent phase, and the often-low selectivity of extraction [22]. Combined UAE-Soxhlet extraction (UAES) has been reported to be a potential method to increase the yield and quality of oils. With recoveries and chemical compositions comparable to those obtained by conventional Soxhlet method and no discernible differences in terms of quality, sono-Soxhlet extraction can be regarded as a novel technique that provides a quick method for the extraction of lipid content [5,16]. According to Luque-Garca and Luque De Castro [16], the official ISO method of sono-Soxhlet extraction has been able to attain efficiencies comparable to or better than those offered by both conventional Soxhlet extraction and UAE, saving both time and sample manipulation. The authors concluded that after applying ultrasound, the composition of the fat extracts remained the same and the precision was comparable to that obtained using the ISO reference technique. Sono-Soxhlet procedures for obtaining oil from the seeds of passion fruit have not been investigated.

Modelling can be used to forecast the extraction process well. The different types of mathematical modelling have been used in the field of food engineering, but the so-called phenomenological or thermodynamic models, which are based on irreversible thermodynamics, have garnered particular attention [21]. It has already been discussed in several publications how the phenomenological model might be used to extract the targeted compounds from plant materials such as resinoids from aerial parts using UAE [19], essential oils from Congo-Brazzaville using hydro-distillation [30], and juniper essential oils using microwave hydro-distillation [18]. The use of phenomenological or thermodynamic models to comprehend the extraction process of sono-Soxhlet

procedures has been the subject of limited research. In this context, this study is justified considering the scarce information and knowledge about the sono-Soxhlet based oil extraction kinetics from passion fruit seeds and its characteristics.

The present chapter dealt with Soxhlet, UAE, and UAES of oil from PFS. The effects of solid-liquid ratio, temperature, and time of UAE treatment on the yield of PFSO were investigated and optimized based on extraction yield. Phenomenological kinetics model was used to understand the extraction phenomena of oil using sono-Soxhlet technique, and physicochemical characterization of optimized sono-Soxhlet extracted oil was performed.

5A.2. Materials and Methods

5A.2.1. Sample preparation

The passion fruit (*Passiflora edulis*) (Yellow) was collected from a local farmer in Manipur, India. Seeds obtained from the fruits as mentioned in **Chapter 3,** were dried in an oven at 50 ℃ until their weights remained constant. Standards used for HPLC were purchased from Sigma. All other chemicals were of analytical grade.

5A.2.2. Ultrasonic assisted extraction (UAE) of oil from Passion fruit seed (PFS)

Coarsely ground dried passion fruit powder was added to the extraction solvent and placed in the ultrasonic bath. The following extraction conditions were investigated for optimization: solid-solvent ratio, extraction temperature, and number of extractions. After extraction, the solution was reduced in a rotary evaporator, and the solvent was recovered. The residue was dried to a constant weight in a vacuum drier to obtain passion fruit seed oil. The passion fruit seed oil was weighed, and the extraction oil yield was calculated.

For the optimization of solid-solvent ratio, 5, 10, 15, 20, 25 and 30% solid-solvent ratio was selected, and all extractions were performed for 30 min at 60 ℃ and the ratio at which the maximum yield of oil occurred was selected as the optimized condition. Similarly, for the selection of temperature, UAE was performed between 30 and 80 ℃ at each 10 ℃ interval at optimized solid-solvent ratio for 30 min of treatment. For extraction time, kinetics calculation experiment was conducted at the optimized solid-solvent ratio and temperature conditions. For all experiments, yield of oil was measured in triplicates.

5A.2.3. Soxhlet method of oil extraction

Soxhlet extraction was selected as conventional extraction technique using ethanol as solvent. The optimized solid-solvent ratio was chosen for each extraction process. The calculated amount of coarsely ground dried PFS was packed in Soxhlet extraction thimbles and inserted in the Soxhlet apparatus and then the required amount of solvent was added, and the system was heated until the boiling of solvent started. The oil was extracted for 8 h, and oil yield was calculated at 10, 20, 30, 60, 90, 120, 180, 240, 300, 360, 420, and 480 min. After the completion of the extraction, the solution was reduced in a rotary evaporator, and the solvent was recovered. The residue was dried to a constant weight in a vacuum drier to obtain passion fruit seed oil. The passion fruit seed oil was weighed, and the yield of extracted oil was calculated.

5A.2.4. Dual UAE-Soxhlet extraction (UAES) of oil from PFS

Optimized UAE condition was followed by Soxhlet extraction for up to total 4 h and its kinetics was studied in terms of oil yield.

5A.2.5. Proximate analysis of PFS

Proximate analysis of passion fruit seed such as moisture, total lipids, crude fiber, crude protein, and ash were measured using standard procedures.

5A.2.5.1. Moisture content of PFS

Moisture content was measure by hot air oven method [26]. Briefly, 2.0 g of sample was weighed into already weighed measured dish and placed it in 105 ℃ oven overnight (with lid was opened until a constant weight loss). The lid was closed and the dish was removed and placed in a desiccator and allowed to cool. Using **Eq. 5A.1,** moisture content was calculated.

$$\text{Moisture content (\%)} = \frac{\text{Weight of fresh sample} - \text{Weight of dry sample}}{\text{Weight of fresh sample}} \times 100 \qquad (5A.1)$$

5A.2.5.2. Total ash content of PFS

The total ash content was determined using modified method described by Ranganna [26]. A minimum of 10 g of samples were taken in pre-weighed crucibles and initially dried in hot air oven 100 ℃ for 1 h, and then placed in a muffle furnace (Thermotech, TIC-4000) and the samples were incinerated at 600 ℃ for 4 h. It was calculated as **(Eq. 5A.2)**

$$\text{Ash} = \frac{(\text{Final weight of crucible after incineration} - \text{weight of empty dried crucible}) \times 100}{\text{Initial volume of sample taken}} \qquad (5A.2)$$

5A.2.5.3. Protein content of PFS

Crude protein content was determined by using Kjeldahl method, which consists of digestion, distillation, and titration steps. **Digestion:** Briefly**,** 0.5 g samples were weighed and transferred to the Kjeldahl flask of the digestion apparatus. Then 15g of mix of potassium sulphate and catalyst (copper (II) sulphate pentahydrate) and 12 mL of sulphuric acid were added to the sample. The solution was boiled till it became clear and light greenand then left to cool. **Distillation into boric acid:** Distillation was performed using boric acid and ammonia was liberated by the addition of the sodium hydroxide solution and collected in the distillate. **Titration:** The distillate was titrated with hydrochloric acid. For the blank test, instead of sample only reagents (no sample was added) was used. Crude protein content was measured using **Eq. 5A.3.**

$$\text{Crude protein content (g/100 g)} = \frac{(V_t - V_{b)}.C_{HCl}.M_N}{w} \times 6.25 \times 100 \quad (5A.3)$$

Where, V_t and V_b are the volume of standard HCl solution used when titrating sample and blank, respectively. C_{HCl} represents the concentration of HCl (mol/L), M_N-nitrogen molar mass (g/mol) and w-nitrogen molar mass (g/mol).

5A.2.5.4. Crude fibre content of PFS

Crude fibre content was measured according to Rangana [26] with modification. Briefly, 3 g protein and oil free sample residues was boiled with concentrated sulphuric acid (1.25 %) for 30 min. Then filtered the suspension of sample through the fritted glass crucible and washed the residue with three consecutive 30 mL portions of boiling water, ensuring that the residue was filtered after each wash. Then treated the sample with concentrated sodium hydroxide (1.25 %) and boiled vigorously for 30 min, washed the residue in the crucible with water and dried in a crucible to constant weight in the oven at 105 ℃. Crude fibre was calculated g/100 g seed.

5A.2.5.5. Total fat content of PFS

Fat content was measured using the same method as described in **Chapter 3**.

5A.2.5.6. Yield of oil

Yield of oil was measured using **Eq. 5A.4.**

$$\text{Oil yield} = \frac{Y_i - Y_f}{Y_i} \quad (5A.4)$$

Where, Y_i and Y_f are the initial and extracted dried residual weight of passion fruit seed powder (g), respectively.

5A.2.6. Physicochemical properties of PFS oil

Physical characterisation was carried out for the seed oil samples. Density measurement was performed using weight and volume of oil. The refractive index was measured at 25 ℃ using hand refractometer.

To evaluate the quality of oil, the conventional and optimized extracted oil samples were analysed for acid value (AV) [8], peroxide value (PV) [8,11] and conjugated diene value (CDV) [8] with some modification. Detailed methods are mentioned in **Chapter 3**.

5A.2.7. Total carotenoid content (TCC) of passion fruit seed oil (PFSO)

TCC of oil extracted samples was determined spectrophotometrically using UV-visible spectrophotometer (CECIL 7400, 700 series, Aquarius) reading absorbance at 450 nm against the used oil as blank [6,11]. Detailed method is mentioned in **Chapter 3.**

5A.2.8. Total phenolic content and HPLC analysis of phenolic acid in PFSO

Folin–Ciocalteu reagent colorimetric method was used for determination of total phenolic content of oils [6]. Detailed method is mentioned **Chapter 3.**

Extracted sample was prepared by taking 5 g samples and mixed with 10 mL methanol and sonicated for 10 min in a bath-sonicator. Then the solvent was separated using centrifuge at 7000 rpm for 10 min. The phenolic acid in the extract was determined according to the method described by Espin et al. [7] using HPLC instrument (UltiMate 3000, Thermo Scientific) with C18 column at column temperature of 35 ℃. Solvents used were 0.1 % formic acid (A) and acetonitrile (B). The elution gradient established was isocratic 15 % B for 5 min, 15–20 % B over 5 min, 20–35 % B over 10 min, 35–50 % B over 10 min, 50–60 % B over 5 min, isocratic 60 % B for 5 min. Overall, the flow rate was 0.5 mL/min and absorbance was read at 280, 330 and 370 nm. Phenolic acids were identified against standards and quantified.

5A.2.9. Fatty acids composition

Fatty acid profiles of the oil samples were determined by methods described by Pereira et al. [22] with some modification. For this study, at first fatty acid methyl ester (FAME) of PFSOs was prepared by following the method described by Purohit et al. [23] with slight modifications. Briefly, 500 mg of oil was mixed with 5 mL of 0.5 N methanolic KOH and was saponified for 5 min at 60 ℃. Then, 15 mL of esterification solution (ammonium chloride and sulphuric acid solution in methanol) was added and the entire mixture was further refluxed for 5 min at 60 ℃. Then the mixture was rinsed

thrice in a separating funnel containing 25 mL petroleum ether and 50 mL water. Finally, the petroleum ether fraction was evaporated to produce the FAME.

The FAMEs were identified by gas chromatography (GCMS-MS) (Model: GCMS-TQ8040, SHIMADZU) according to Pereira et al. [22]. The carrier gas was nitrogen used with a constant flow rate of 2.0 mL/min. Temperature of the injector and detector was set at 260 ℃ and 300 ℃, respectively. The following procedure was followed: Started oven temperature at140 ℃ for 40 min followed by ramping the temperature to 240 ℃ at rate of 2 ℃/min and remained at this temperature for the entire time of analysis. After dilution with chromatographic-grade n-hexane (ratio 1:100), a sample of methyl esters was injected in a split mode. FAMEs were identified by comparison with retention times of the standard mixture FAMEs (Supelco, MIX FAME 37, St. Louis, MO 63103, USA). Each fatty acid was quantified as percentage of total methyl ester peak areas.

5A.2.10. Calculated oxidizability (COX) value

COX value was calculated according to the following formula that is used on the unsaturated fatty acids (C18) [3,23] **(Eq. 5A.5).**

$$\text{COX value} = [\text{C18:1\%}+\{10.3\times \text{C18:2(\%)}\}+\{21.6\times \text{C18:3(\%)}\}]\div 100 \qquad (5A.5)$$

Where, C18:1, C18:2 and C18:3 represent the oleic acid, linoleic acid, and linolenic acid, respectively.

5A.2.11. Antioxidant activity

5A.2.11.1. DPPH (2,2-diphenyl-1-picrylhydrazyl) radical scavenging activity

DPPH antioxidant activity determines the hydrogen donating capacity of molecules and does not produce oxidative chain reactions or react with free radical intermediates [22].

DPPH free radical activity of sample was determined by using the same methods described by Chutia et al. [1] with slightly modification, which is mentioned in **Chapter 3** in details.

5A.2.11.2. The 2.2-Azino-bis (3-ethylbenzothiazoline-6-sulfonic acid) diammonium salt (ABTS) activity

ABTS of the sample oils was identified using the method given by Pereira wt al. [22] with some modifications. ABTS reaction solvent was prepared from the reaction of 7 mM of ABTS solution with 2.45 mM of potassium persulfate. The mixture was then kept in the dark at room temperature for 16 h. At the time of use, the ABTS reaction

solvent was diluted with spectrometric grade ethanol to yield an absorbance of 0.70 ± 0.02 at 734 nm. Then, 20 μL oil samples were mixed with 230 μL ABTS reactive solvent. The mixture was mixed properly and kept undisturbed for 6 min and the absorbance at 734 nm was noted. Results were expressed as Trolox Equivalent Antioxidant Capacity (TEAC). A distinct concentration response curve for standard Trolox solutions was created to determine TEAC values.

5A.2.12. Phenomenological kinetics model

Among the various kinds of mathematical modelling used in food engineering, the so-called phenomenological or thermodynamic models, which is based on Irreversible Thermodynamics is of special interest [21]. The mathematical model was based on the following assumptions [18,19]: (A) The extracted materials oil was considered to be a pseudo-single component; (B) Perfectly mixed solution was in the system; (C) Plant matrices were isotropic in nature and equal in shape, size, and initial oil content; (D) The fractions of the oil extracted via washing ($-k_1$), unhindered diffusion ($-k_2$) and hindered diffusion ($-k_3$) were assumed to be constant; (E) Negligible resistance to the mass transfer from the plant matrices; (F) A fraction of the oils was located at the external surfaces (F) and rest was uniformly distributed in the matrices (1-f); (G) The extraction process occured via two simultaneous mechanisms: (i) Rapid penetration of solvent and dissolution of the oil located on or near surfaces of solid matrices known as washing, and (ii) mass transfer of oil soluble compounds from the plant matrices into the extractable solvent by diffusion and osmotic processes that are well known as slow extraction; (H) Both processes were exponential and occurred simultaneously from the beginning; (I) The fractions of oil extracted *via* washing, unhindered diffusion and hindered diffusion (f1, f2 and f3, respectively) were assumed to be constant **(Eq. 5A.6);**

$$-\frac{dw_p}{dt} = k \times w_p \quad (5A.6)$$

Where, w_p was the average content of oil in the plant particles (g/100 g) at time 't', and process rate constant (k).

For, t = 0, $w_p = w_\infty$, so the integration of **Eq. 5A.6** gave the following expression for washing, unhindered diffusion, and hindered diffusion, respectively (**Eq. 5A.7-9**)

$$\frac{w_{p,1}}{w_\infty} = \exp(-k_1 t), \quad \frac{w_{p,2}}{w_\infty} = \exp(-k_2 t), \quad \frac{w_{p,3}}{w_\infty} = \exp(-k_3 t) \quad (5A.7)$$

Based on the assumption,

$$\frac{w_p}{w_\infty} = f1 \times \exp(-k_1 t) + f2 \times \exp(-k_2 t) + f3 \times \exp(-k_3 t) \quad (5A.8)$$

Where, $f1 = \frac{w_{p,1}}{w_\infty}$, $f2 = \frac{w_{p,2}}{w_\infty}$ and $f3 = \frac{w_{p,3}}{w_\infty}$, and, $f1 + f2 + f3 = 1$

Hence, the amount of essential oil extracted until time 't', $w = w_\infty - w_p$ follows

$$\frac{w}{w_\infty} = 1 - f1 \times \exp(-k_1 t) - f2 \times \exp(-k_2 t) - f3 \times \exp(-k_3 t) \quad (5A.9)$$

Or

$$w = w_\infty(1 - f1 \times \exp(-k_1 t) - f2 \times \exp(-k_2 t) - f3 \times \exp(-k_3 t)) \quad (5A.10)$$

It was assumed that hindered diffusion was negligible ($f3 = 0$), model can be represented by **Eq. 5A.11:**

$$w = w_\infty(1 - f1 \times \exp(-k_1 t) - (1 - f1) \times \exp(-k_2 t) \quad (5A.11)$$

if washing was faster than diffusion, ($k_1 \gg k_2$), then **Eq. 5.12** follows:

$$w = w_\infty[1 - (1 - f1)\exp(-k_2 t) \quad (5A.12)$$

if f=0, which implies that washing does not occur

$$w = w_\infty[1 - \exp(-k_2 t) \quad (5A.13)$$

Here. **Eq. 5A.11**, **Eq. 5A.12** and **Eq. 5A.13** represent the Phenomenological model, pseudo first order model and Model based on instantaneous washing followed by diffusion, respectively.

5A.2.13. Statistical analysis

The model parameters were estimated using MATLAB 7.14 (Release 2012a) and non-linear least squares regression using Microsoft Excel Solver (Microsoft office, USA). The performances of the developed model were statistically measured by coefficient of determination (R^2), mean squared error (MSE), and mean relative percent deviation (MRPD %), which were calculated using the following equations **(Eq. 5A.14-16):**

$$R^2 = 1 - \frac{\sum_{i=1}^{N}(Z_{pre} - Z_{exp})}{\sum_{i=1}^{N}(Z_{mean} - Z_{exp})} \quad (5A.14)$$

$$MSE = \frac{1}{n}\sum_{i=1}^{N}(Z_{exp} - Z_{pre})^2 \quad (5A.15)$$

$$MRPD = 1 - \sum_{i=1}^{N} \left| \frac{(Z_{pre} - Z_{exp})}{(Z_{exp})} \right| \quad (5A.16)$$

Where, Z_{Exp}, $Z_{Pre,}$ and Z_{mean} represent the experimental, predicted and mean values of the data respectively, N is the number of data sets (n = 1, 2, 3,. . . ,N).

5A.3. Results and Discussion

5A.3.1. Proximate analysis of PFS

The results of proximate analysis of PFS are reported in **Table 5A.1.** After drying, the moisture content was 8.64 %, whereas reported moisture content of yellow passion fruit seed varied from 7.38-12.38 % [17,23]. Purohit et al. [23] observed that the moisture content of dried yellow PFS samples cultivated in Assam and Manipur was 12.38 % and 12.34 %, respectively, whereas Malacrida and Jorge [17] reported about 7.38 % moisture content in PFS cultivated in Brazil.

Table 5A.1. Proximate analysis of passion fruit seeds.

Parameters	Amount
Moisture (g/100 g)	8.64±0.64
Total lipids (g/100 g)	24.4 ±2.78
Crude fiber (g/100 g)	51.59±3.81
Crude protein (g/100 g)	11.58±0.87
Ash (g/100 g)	1.64±0.18

The oil content was 24.4%. In comparison, Purohit et al. [23] found 24.6 and 28% oil in PFS cultivated in Manipur and Assam, respectively, and Malacrida and Jorge [17] obtained 30.39% oil in Brazilian yellow PFS. Dos Reis et al. [27] observed 12.31% to 19.64% oil content in PFS. Giuffre [10] reported 22.40 % oil in purple PFS. PFS contained crude fibre (51.59 g/100 g), crude protein (11.58 g/100 g), and ash content (1.64 g/100 g), which agreed with the previous reports [17,20,22,23,25]. Oliveira et al. [20] observed 46 % raw fiber, 13.2 % crude fibre, 24.8% total lipid in yellow PFS grown in Brazil, whereas Malacrida and Jorge [17] found 7.38 % moisture content, 30.39 % lipid, 12.23 % protein, 1.75 % ash, and fibre 48.73% in Brazil- based yellow PFS. Diverse geoclimatic conditions may be the cause of variations in physicochemical characteristics.

5A.3.2. Effect of the solid-liquid ratio on ultrasonic extraction of PFSO

The best oil yield is achieved when the solution reaches saturation concentration. In our study, the solid-solvent ratio varied between 5 and 30 %. The yield of oil increased rapidly up to a solid-liquid ratio of 20 %, after which slight increase in yield was only observed. At 20 % solid-liquid ratio, 75.6 % of total oil was extracted by UAE, any further increase in the ratio increased the oil yield only marginally **(Fig. 5A.1a**). Therefore, a solid-liquid ratio of 20 % was selected as the optimized ratio for further

tests. UAE extraction of oil from tara seed was conducted using petroleum ether at liquid-solid ratio from 8:01-16:01 and 14:01 was reported as the optimum ratio [15]. Goula et al. [11] also reported similar trends for carotenoids extraction using UAE.

5A.3.3. Effect of extraction temperature on ultrasonic extraction of PFSO

UAE temperature affects the interaction between the solid and liquid. When the ultrasonic temperature was increased from 30 to 70 ℃, the yield of oil increased from 62.4 % to 81.3 % **(Fig 5A.1b**), whereas extraction at 80 ℃ caused slight decrease (0.1 %) in yield. Therefore, 70 ℃ was selected as the optimum temperature for subsequent experiments. Solvent and oil viscosity decreases as temperature rises, improving its fluidity and facilitating its flow through solid matrices as well as raising the diffusion coefficients of the compounds that can be extracted from lipophiles. But at temperatures >70 ℃, dissolution of cell impurities and decomposition of some constituents may increase, and too high temperatures would enhance the speed of bubble collapse in the solvent, which may hamper the strength of the bubbles, and thus decrease the yield [11].

5A.3.4. Effect of extraction time on ultrasonic extraction of PFSO

Extraction times varying between 5 and 90 min were used to investigate the effect of oil yield (**Fig 5A.1c),** and the extraction yield was observed to increase with time. This might be because greater time allows the ultrasonic wave to penetrate cell walls and release the cell contents. The extraction yield was rapid up to around 30 min and thereafter the rate slowed down, which was also reported by Raj and Dash [24]. To extract approximately 75% of total oil, it required approximately 30 min and to extract the next 12 % oil, it required another 60 min. So, 30 min was chosen as the optimized UAE time.

5A.3.5. Soxhlet extraction of PFSO

It is evident that when treatment time was extended at a steady temperature, extracted oil yield rose until it reached saturation (**Fig 5A.2a**). Higher yield is a result of the solvent's viscosity being reduced, the extracted oil being more fluid and soluble, and the solvent's diffusivity and mass transfer being improved. Similarly, higher the treatment time means prolonged contact or exposure with the solvent [11]. To extract approximately 50 % total extractable oil, it required approximately 120 min, to extract the next 30 % oil approximately another 2 h was required. For further 20 % extraction yield, it required another 4 h.

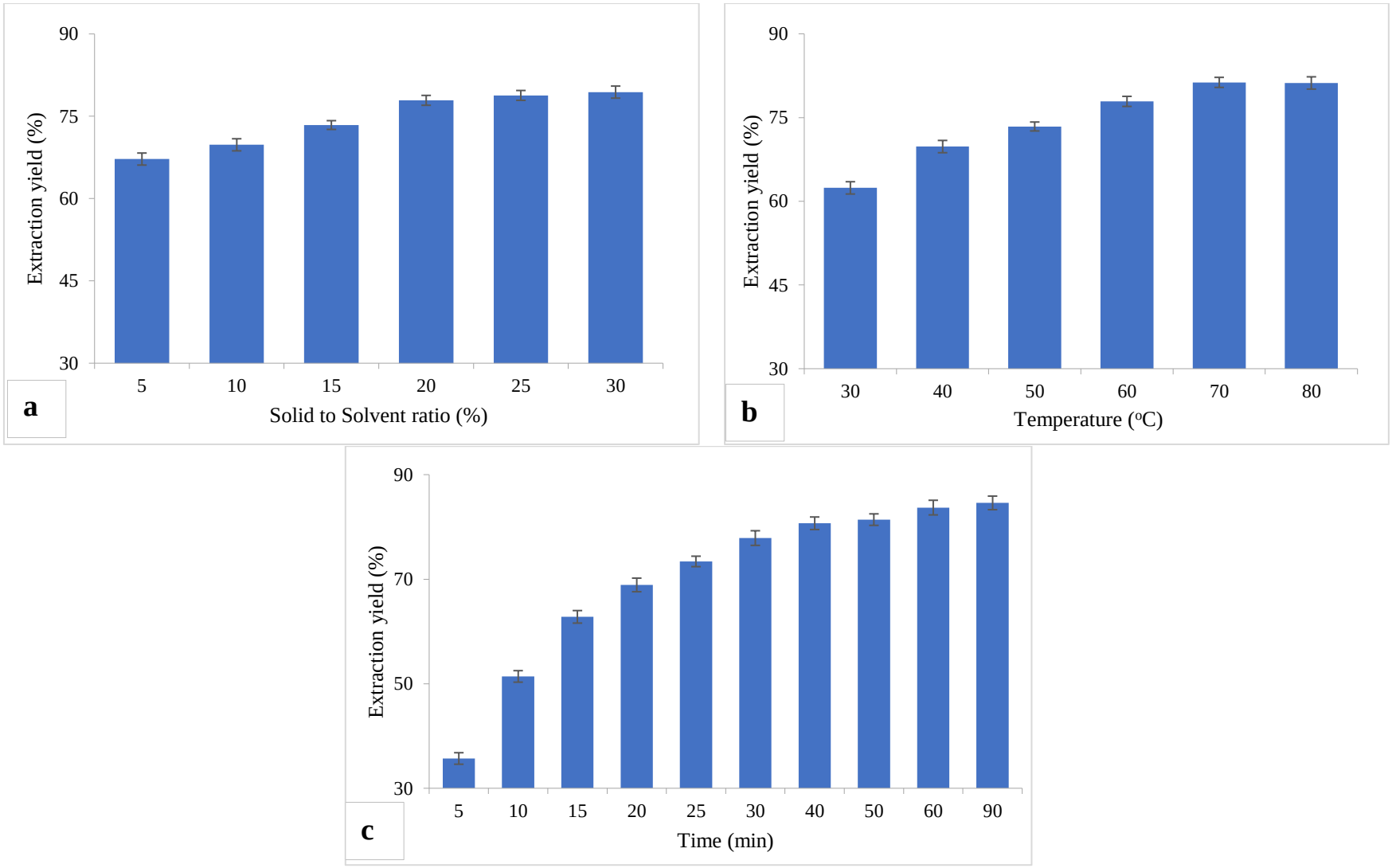

Fig. 5A.1. Effect of extraction parameters on extraction yield of passion fruit seed oil: (a) Solid-solvent ratio, (b) Temperature, and (c) Time.

5A.3.6. UAE-Soxhlet extraction of PFSO

In this extraction process, optimized UAE extraction was performed for first 30 min followed by Soxhlet extraction for 4 h **(Fig 5A.2a).** The results revealed that combined UAE-Soxhlet extraction was able to extract approximately 95% of oil within a short period of time (4 h), which otherwise using Soxhlet extraction process would approximately require 8 h to extract 95% of total oil. Using UAE only, it was very difficult to extract more than 85% of the total oil. The overall improvement may be due to the synergistic effect of ultrasound and Soxhlet extraction processes.

5A.3.7. Kinetic modelling of extraction of PFSO

Fig. 5A.2b illustrates the variation of the oil yields with different extraction techniques from PFS using ethanol as the solvent. For all extraction processes, oil yield increased with extraction time. Using UAES process, overall extraction rate was higher as compared to Soxhlet and yield was higher as compared to UAE. The positive and synergetic effect of UAES process on extraction yield may be because UAE disrupted the cell wall and enhanced the accessibility of oil, and the later use of higher temperature in Soxhlet method decreased the viscosity of the solvent and enhanced the overall fluidity [5] and solubility of the oil and as a result it enhanced the diffusivity and mass transfer [12].

This study suggested that combined ultrasound and Soxhlet with ethanol as solvent can be used as a novel technology for higher extraction efficiency with short time period. UAE followed by Soxhlet extraction can be easily scaled up for industrial use as a food processing technique, with good product quality and high returns on capital investment [4]. The oil extraction mechanism from PFS consisted of two stages. In the initial stage, rapid extraction of the extractable materials located at the surfaces occurred, and then the extractable materials from intact cells slowly diffused to the surface of the particles [18,30]. This observation was very important for subsequent modelling of the extraction kinetics.

5A.3.8. Phenomenological model

The kinetics of oil by UAE, Soxhlet, and UAESO was described by phenomenological models that are represented in **Table 5A.2.** Values of the model parameters of **Eq. 5A.11** and the statistical criteria used for assessing the goodness of fit (R^2, MRPD, and MSE) are presented in **Table 5A.2**. The experimental and predicted values of the oil yield agreed very well with each other **(Fig. 5A.2c)** as high coefficient

of determination (R^2> 0.9971), low MSE (<0.1118) and the acceptable MRPD (<±1.7892–1.5521 %) implied the good fitting that explained the extraction phenomena on using the phenomenological model. This can be visually observed in **Fig. 5A.2b**. The oil yield at saturation point increased with extraction techniques, which may be due to the increase in the extraction temperature as Soxhlet extraction temperature was higher than UAE. The fraction of washable extractable substances was decreased with increase in the extraction temperature, for both Soxhlet and UAE extraction techniques. The "f1" values were higher for the UAE (0.7320) followed by combined UAESO (0.7259) and Soxhlet extraction (0.0096) (**Table 5A.2**), which demonstrated the influence of ultrasound on the washing extraction process [19,20].

k_1 and k_2 values for all extraction process ranged from 0.0807 to 0.1139 min^{-1} and 0.0050 to 0.0054 min^{-1}, respectively, and for all extraction process $k_1 >> k_2$, which indicated the predominance of the washing process. k_1 value for UAE extraction process was higher than Soxhlet extraction process, whereas k_1 value was highest for UAESO extraction, which indicated the synergistic effect of UAE and Soxhlet on the washing process as well as the overall extraction process. Milic et al. [19] observed similar trend for UAE and conventional extraction processes. Marković et al. [18] found similar values for phenomenological model parameters where k_1 was 0.1753 min^{-1}, k_2 was 0.0173 min^{-1} and f1 was 0.619 during the extraction of essential oil from juniper.

Two simpler models were developed, namely the pseudo-first order model **(Eq. 5A.12),** where washing process was neglected, and the model based on instantaneous washing followed by diffusion, where diffusion process was neglected (**Eq. 5A.13).** These models were evaluated for the purpose of comparison with the phenomenological model (**Eq. 5A.11).** The kinetics parameters of these two simpler models are presented in **Table 5A.3.** The k_2 value of pseudo first order model ranged between 0.0083 and 0.0754 min^{-1}, whereas the same parameter value for model based on instantaneous washing followed by diffusion ranged from 0.0081-0.0714 min^{-1} **(Table 5A.3).** For each extraction process, k_2 value of pseudo first order model was found higher than the model based on instantaneous washing followed by diffusion process.

The pseudo-first order model and instantaneous washing followed by diffusion model had small R^2 value and relatively high MSE and MRPD (%) values as compared to phenomenological model, independently for the adopted extraction techniques.

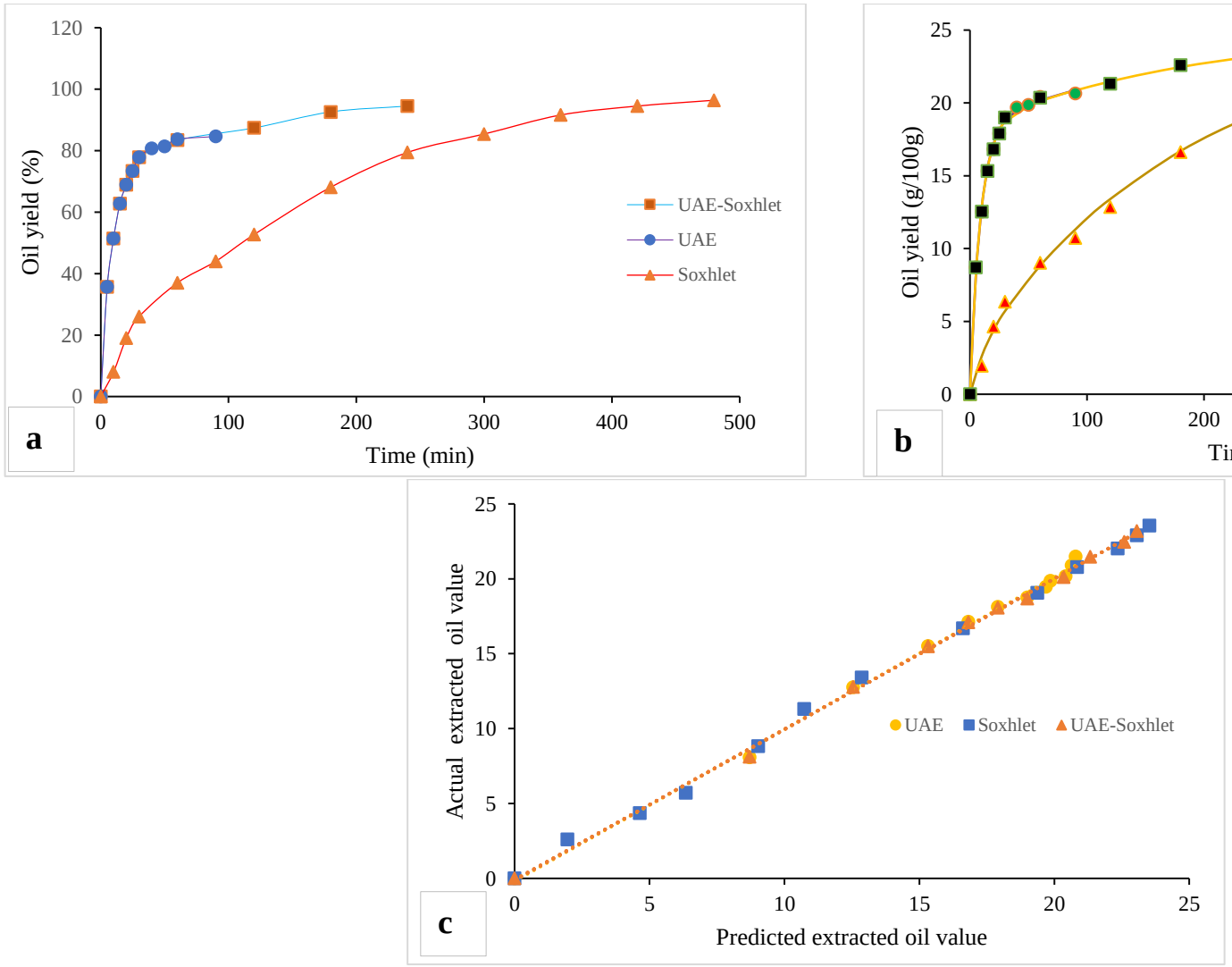

Fig. 5A.2. UAE, Soxhlet, and UAES of oil: (a) Extraction oil yield, (b) Phenomenological modeling kinetics, (c) Predicted and Actual value of yield oil.

Table 5A.2. Phenomenological model parameters for extraction of oil from passion fruit seeds.

Extraction	$\mathbf{w_\infty}$	**f1**	$\mathbf{k_1\ (min)^{-1}}$	$\mathbf{k_2\ (min)^{-1}}$	$\mathbf{R^2}$	**MRPD (%)**	**MSE**
UAE	22.3 ± 1.6	0.7320± 0.04	0.1121 ± 0.009	0.0050 ± 0.0008	0.9971	± 1.7892	0.1118
Soxhlet	25.2 ± 1.0	0.0996 ± 0.08	0.0807 ± 0.003	0.0054 ± 0.0005	0.9979	± 5.0331	0.1386
UAE-Soxhlet	24.7 ± 1.4	0.7259 ± 0.07	0.1139 ± 0.007	0.0051 ± 0.0007	0.9984	± 1.5521	0.0690

Table 5A.3. Parameters of pseudo-first order model and model based on instantaneous washing followed by diffusion for extraction of oil from passion fruit seeds.

Extraction	**Pseudo first order**				**Model based on instantaneous washing followed by diffusion**				
	$\mathbf{k_2\ (min)^{-1}}$	$\mathbf{R^2}$	**MRPD (%)**	**MSE**	**f**	$\mathbf{k_2\ (min)^{-1}}$	$\mathbf{R^2}$	**MRPD (%)**	**MSE**
UAE	0.0727 ± 0.0007	0.9951	± 6.9015	1.5887	0.0582± 0.05	0.0676	0.9778	± 5.8780	1.4167
Soxhlet	0.0083 ± 0.0004	0.9869	± 7.9713	0.9881	0.0245 ±0.03	0.0081	0.9885	± 7.4399	0.9257
UAE-Soxhlet	0.0754 ± 0.0007	0.9837	± 4.6175	0.9357	0.0451± 0.04	0.0714	0.9827	± 4.6175	0.8257

Therefore, only pseudo first order model and instantaneous washing followed by diffusion models were less efficient as compared to dual extraction (phenomenological model) for describing the extraction kinetics of oil from PFS, Thus, the phenomenological model better explained the variation of oil yield than the simpler models and could be recommended for modelling the extraction kinetics.

5A.3.9. Physicochemical properties of PFSO

Pereira et al. [22] mentioned that the oil extracted using *n*-hexane was transparent and almost without coloration whereas the oil extracted using ethanol showed yellow coloration. The physicochemical properties of UAES and Soxhlet extracted PFSOs were calculated and are reported in **Table 5A.4**. The acid values of the oils extracted by optimized UAESO and Soxhlet method were 2.40 and 2.81 mg KOH/g oil, respectively (**Table 5A.4**), which was within the permissible limit of 4.0 mg KOH/g for crude oil set by Codex Alimentarius International [2]. Acid value of 2.0 and 4.8 mg KOH/g for PFSO was reported by Purohit et al. [23]. The higher acid value for Soxhlet may be due to the prolonged heat treatment [23]. Similarly, the peroxide value of the extracted oils was within the permissible range.

Table 5A.4. Physicochemical properties of passion fruit seed oil.

Parameters	**UAESO**	**Soxhlet extracted oil**
Acid value (mg KOH/ g oil)	2.40±0.07	2.81±0.09
Iodine value (g I_2/100 g)	130.22±0.50	139.41±0.70
Peroxide value (mg Eq O_2/100g)	4.80±0.04	5.20±0.07
Refractive Index (at 25ºC)	1.47±0.01	1.54±0.02
Density (g/L) (at 25ºC)	918.25±0.72	902.18±0.91
Induction time (h)	2.42±0.07	2.14±0.08
Total phenolic content (mg GAE/g of oil)	28.97±0.70	26.87±0.90
Total carotenoids (µg ß-carotene/g)	5.80 ±0.04	5.11±0.02
DPPH scavenging activity (%)	71.28±1.45	67.80±1.24
ABTS activity (µM TEAC/g oil)	172±3.50	139±4.12

Between the two extraction methods, the UAES extracted oil demonstrated better oil quality. Low acid value and peroxide value of PFSO suggested the good quality and edibility of the oil. The scent and flavour of the oil are produced by free fatty acids. The percentage of unsaturated substance in oil is determined by the iodine value of the oil [23]. For combined UAESO extraction, the iodine value of passion fruit seed oil was

determined to be 130.22 g I_2/100 g oil, and for Soxhlet extraction it was 139.41 g I_2/100 g oil **(Table 5A.4).**

Purohit et al. [23] discovered the iodine value to be between 126.9 and 131.4 for yellow passion fruit seed oil. The PFS possessed high values of iodine (124.67±0.67-131.00±0.58 g I_2/100 g) and peroxides (1.43±0.12-3.23±0.12 meq O_2/kg) similar to other edible seed oils reported by Ramaiya et al. [25]. The refractive index of PFSO from UAESO and UAE extraction was 1.47 and 1.54, respectively **(Table 5A.4),** which is within the range of refractive index for most vegetable oils [2]. Refractive index for sweet PFSO extracted using ethanol as solvent with ultrasonication assisted extraction was 1.4678 at 40 ℃ and 1.4743 at 20 ℃ [22]. This value indicated the presence of long-chain unsaturated fatty acids and also intermolecular interaction in PFSO [23]. Density of UAES oil was found to be higher than Soxhlet extracted oil. The lower antioxidant activity observed in this study may be attributed to the high temperature used for extraction in the Soxhlet apparatus [25].

Total carotenoids content of oil treated by UAESO and Soxhlet was 5.8 and 5.11 µg β-carotene/g of oil, respectively, where ß-carotene is the major carotenoid in the seed oils. Similarly, 6.70 µg β-carotene/g sample of oil was reported by da Silva and Jorge [31]. Total phenolic content, total carotenoids content and overall antioxidant activity of oil extracted by UAESO technique was higher as compared to Soxhlet process. Prolonged heating in Soxhlet may degrade the total phenolic content and total carotenoids, which affects the overall antioxidant activity of the oil [11].

Total phenolic content in passion fruit seed oil was 33.57 mg GAE/g of oil, whereas 36.02-39.11 mg GAE/g of total phenolic content in yellow passion fruit seed oil from North East region was reported by Purohit et al. [23]. Four major phenolic compounds were detected by HPLC method, namely gallic acid (20 %), salicylic acid (16.4 %), piceatannol (54.6 %) and kaempferol (8 %). da Silva and Jorge [31] found caffeic acid, coumaric acid and salicylic acid, with salicylic acid being the major phenolic acid. de Santana et al. [29] identified stilbene, piceatannol as the major compounds in yellow passion fruit seed extract, which accounted for 50 % of total phenolic content.

5A.3.10. Fatty acids composition

The fatty acid composition and its relative percentage of optimized extracted yellow PFSO are presented in **Table 5A.5**. The FAME composition of oils indicated the

presence of unsaturated fatty acids, which was also observed from high iodine value. Moreover, in this study, refractive index indicated long chain unsaturated fatty acids in the PFS, which was confirmed by the presence of high amount of linoleic acid and oleic acid. The major fatty acids found in PFSO were linoleic acid (67.3 %), oleic acid (16.1 %), palmitic acid (13.4 %), stearic acid (2.5 %), and linolenic acid (0.58 %).

Table 5A.5. Fatty acid composition of UASEO.

Parameters	**Amount**
Palmitic acid (C16:0, %)	13.4
Stearic acid (C18:0, %)	2.5
Oleic acid (C18:1, %)	16.1
Linoleic acid (C18:2, %)	67.3
Linolenic acid (C18:3, %)	0.58
Saturated fatty acid (SFA, %)	15.9
Unsaturated fatty acid (UFA, %)	84.0
Monounsaturated fatty acid (MUFA, %)	16.1
Polyunsaturated fatty acid (PUFA, %)	67.9
COX value	7.2

The total content of saturated fatty acids (SFA) was 15.9 %, while the content of unsaturated ones (UFA) was 84 %. Palmitic acid was predominant among the SFAs. The results agreed with the report of Purohit et al. [23] and Pereira et al. [22]. 69.8 % linoleic acid, 13.8 % oleic acid and 13.4 % palmitic acid in yellow PFSO was observed by Purohit et al. [23]. Whereas, fatty acid composition in sweet passion fruit seed were linoleic acid (72.00-72.88 %), oleic acid (12.54-13.25 %), palmitic acid (11.17-11.50 %) and stearic acid (2.47-2.57 %), as observed by Pereira et al. [22].

The COX value for UAES oil was 7.2, which was calculated by considering the percentages of oleic acid, linoleic acid, and linolenic acid present in the PFSO; and higher unsaturated fats leads to an increase in COX value of oils. PFSO was, therefore, stable and can also be employed for prevention of oxidative deterioration. Purohit et al. [23] reported almost similar COX values (7.4) in PFSO. In comparison, COX value of fresh palm oil, peanut oil, camellia oil was 1.615, 4.631, and 1.772, respectively [33].

5A.4. Conclusion

A new and efficient approach based on the dual extraction of passion fruit seed oil in ethanol using ultrasound and Soxhlet methods is proposed. In this study, effect of

solid-solvent ratio, temperature, and extraction time on UAE extraction of PFSO was investigated and optimization was also performed. Using optimized conditions, combination of ultrasound and Soxhlet based techniques was used for the efficient extraction of oil from seed. Study results indicated that combined ultrasound and Soxhlet procedures were effective in extracting the oil from PFSO than Soxhlet (in terms of time consumption) and UAE (in terms of extraction yield). The developed phenomenological model for explaining the kinetics of the extraction process had demonstrated that combined techniques strongly influenced only the washing process. Generalization ability of this kinetics model should not be ignored in future modelling of the extraction kinetics. Phenomenological model better explained the variation of oil yield than the simpler models and could be recommended for modelling the extraction kinetics. The overall quality and yield of oil was found to be better than the oil extracted by the Soxhlet apparatus.

Bibliography

[1] Chutia, H., Mahanta, C. L., Ojah, N. and Choudhury, A. J. Fuzzy logic approach for optimization of blended beverage of cold plasma treated TCW and orange juice. *Journal of Food Measurement and Characterization*, 14(4):1926–1938, 2020.

[2] Codex Alimentarius (International Food Standards). *Standard For Named Vegetable Oils*. CXS 210-19(2): 2019.

[3] Dabetic, N. M. et al. Grape Seed Oil Characterization: A Novel Approach for Oil Quality Assessment. *European Journal of Lipid Science and Technology*, 122(6):1–10, 2020.

[4] Deenu, A., Naruenartwongsakul, S. and Kim, S. M. Optimization and Economic Evaluation of Ultrasound Extraction of Lutein from *Chlorella vulgaris*. *Biotechnology and Bioprocess Engineering*, 1151–1162, 2013.

[5] Djenni, Z., Pingret, D., Mason, T. J. and Chemat, F. Sono-Soxhlet: In Situ Ultrasound-Assisted Extraction of Food Products. *Food Analytical Methods*, 6(4):1229–1233, 2013.

[6] Elik, A., Yanik, D. K. and Göğüş, F. Microwave-assisted extraction of carotenoids from carrot juice processing waste using flaxseed oil as a solvent. *LWT - Food Science and Technology*, 123:109100, 2020.

[7] Espin, S. et al. Phenolic composition and antioxidant capacity of yellow and

purple-red Ecuadorian cultivars of tree tomato (*Solanum betaceum Cav*.). *Food Chemistry*, 194:1073–1080, 2016.

[8] Farhoosh, R., Khodaparast, M. H. H., Sharif, A. and Rafiee, S. A. Olive oil oxidation: Rejection points in terms of polar, conjugated diene, and carbonyl values. *Food Chemistry*, 131(4):1385–1390, 2012.

[9] García-Hernández, V. M. et al. Comparison of Soxhlet and ultrasound methods for oil extraction from Spanish Flaxseeds. *Journal of Microbiology, Biotechnology and Food Sciences*, 7(3):332–336, 2017.

[10] Giuffre, A. M. Chemical composition of purple passion fruit (*Passiflora edulis Sims var. edulis*) seed oil. *Rivista Italiana Delle Sostanze Grasse ·*, 2007.

[11] Goula, A. M., Ververi, M., Adamopoulou, A. and Kaderides, K. Green ultrasound-assisted extraction of carotenoids from pomegranate wastes using vegetable oils. *Ultrasonics Sonochemistry*, 34:821–830, 2017.

[12] Hlaváč, P., Božiková, M. and Petrović, A. Selected physical properties assessment of sunflower and olive oils. *Acta Technologica Agriculturae 3*(2):86–91, 2019.

[13] Jusuf, N. K., Putra, I. B. and Dewi, N. K. Antibacterial activity of passion fruit purple variant (*Passiflora edulis sims var. edulis*) seeds extract against propionibacterium acnes. *Clinical, Cosmetic and Investigational Dermatology*, 13:99–104, 2020.

[14] Kawakami, S. et al. Constituent characteristics and functional properties of passion fruit seed extract. *Life*, 12(1): 2022.

[15] Li, Z. J., Yang, F. J., Yang, L. and Zu, Y. G. Ultrasonic Extraction of Oil from Caesalpinia spinosa (Tara) seeds. *Journal of Chemistry*, 1794123: 2016.

[16] Luque-García, J. L. and Luque De Castro, M. D. Ultrasound-assisted Soxhlet extraction: An expeditive approach for solid sample treatment - Application to the extraction of total fat from oleaginous seeds. *Journal of Chromatography A*, 1034(1–2):237–242, 2004.

[17] Malacrida, C. R. and Jorge, N. Yellow Passion Fruit Seed Oil *(Passiflora edulis f. flavicarpa*): Physical and Chemical Characteristics. *Brazilian Archives of Biology and Technology*, 55(1):127–134,

[18] Marković, M. S. et al. A new kinetic model for the common juniper essenstial oil extraction by microwave hydrodistillation. *Chinese Journal of Chemical Engineering*, 27(3):605–612, 2019.

[19] Milic, P. S., Rajkovic, K. M., Stamenkovic, O. S. and Veljkovic, V. B. Kinetic

modeling and optimization of maceration and ultrasound-extraction of resinoid from the aerial parts of white lady's bedstraw (*Galium mollugo L.*). *Ultrasonics Sonochemistry*, 20:525–534, 2013.

[20] Oliveira, R. C., G deuedes, T. A., Gimenes, M. L. and de Barros, S. T. D. Effect of process variables on the oil extraction from passion fruit seeds by conventional and non-conventional techniques. *Acta Scientiarum - Technology*, 36(1):87–91, 2014.

[21] Orphanides, A., Goulas, V. and Gekas, V. Introducing the concept of sono-chemical potential : A phenomenological model for ultrasound assisted extraction. *Journal of Food Engineering*, 120:191–196, 2014.

[22] Pereira, M. G., Hamerski, F., Andrade, E. F., Scheer, A. de P. and Corazza, M. L. Assessment of subcritical propane, ultrasound-assisted and Soxhlet extraction of oil from sweet passion fruit (*Passiflora alata Curtis*) seeds. *Journal of Supercritical Fluids*, 128:338–348, 2017.

[23] Purohit, S., Kalita, D., Barik, C. R., Sahoo, L. and Goud, V. V. Evaluation of thermophysical, biochemical and antibacterial properties of unconventional vegetable oil from Northeast India. *Materials Science for Energy Technologies*, 4:81–91, 2021.

[24] Raj, G. V. S. and Dash, K. K. Ultrasound-assisted extraction of phytocompounds from dragon fruit peel: Optimization, kinetics and thermodynamic studies. *Ultrasonics Sonochemistry*, 68: 2020.

[25] Ramaiya, S. D., Bujang, J. S. and Zakaria, M. H. Physicochemical, Fatty Acid and Antioxidant Properties of Passion Fruit (Passiflora Species) Seed Oil. *Pakistan Journal of Nutrition*, 18(5):421–429, 2019.

[26] Ranganna, S. *Handbook of analysis and quality control for fruits and vegetable products*. *Tata McGraw-Hill Education*, 1986.

[27] Reis, L. C. R. D., Facco, E. M. P., Salvador, M., Flôres, S. H. and Rios, A. de O. Antioxidant potential and physicochemical characterization of yellow, purple and orange passion fruit. *Journal of Food Science and Technology*, 55(7):2679–2691, 2018.

[28] Ribeiro, D. N. et al. Extraction of passion fruit (*Passiflora cincinnata Mast*.) pulp oil using pressurized ethanol and ultrasound: Antioxidant activity and kinetics. *Journal of Supercritical Fluids*, 165: 2020.

[29] Santana, F. C. D. et al. Optimization of the antioxidant polyphenolic compounds

extraction of yellow passion fruit seeds (*Passiflora edulis Sims*) by response surface methodology. *Journal of Food Science and Technology*, 54(11):3552–3561, 2017.

[30] Silou, T., Bassiloua, J. B. and Kama Niamayoua, R. Kinetic Modeling of Essential Oil Extraction by Hydrodistillation of *Xylopia aethiopica* (Dunal) A. Rich Fruits from Congo-Brazzaville. *European Journal of Biology and Biotechnology*, 2(3):105–110, 2021.

[31] Silva, A. C. D. and Jorge, N. Bioactive compounds of oils extracted from fruits seeds obtained from agroindustrial waste. *European Journal of Lipid Science and Technology*, 118: 2016.

[32] Teng, H. et al. Ultrasonic-Assisted Extraction of Raspberry Seed Oil and Evaluation of Its Physicochemical Properties, Fatty Acid Compositions and Antioxidant Activities. *PLoS ONE*, 11(4): 2016.

[33] Xu, T. T., Li, J., Fan, Y. W., Zheng, T. W. and Deng, Z. Y. Comparison of oxidative stability among edible oils under continuous frying conditions. *International Journal of Food Properties*, 18(7):1478–1490, 2015.

CHAPTER 5 SECTION B

PROPERTIES OF DIETARY FIBRE FROM PASSION FRUIT SEED OBTAINED THROUGH INDIVIDUAL AND COMBINED ALKALINE AND ULTRASONICATION EXTRACTION TECHNIQUES

5B.1. Introduction

Passion fruit (*Passiflora edulis*) is widely used in traditional medicine throughout the world and is being exploited by the food, pharmaceutical, and cosmetics industries [9]. However, a significant issue with passion fruit juice manufacturing units is the significant amount of waste that is generated from the discarded peels and seeds, which makes up more than half (about 60 %) of the fruit weight [30]. Passion fruit seeds constitute up to 25 % of total fruit weight and are edible [5,30]. The raw seeds of passion fruit are high in crude fat (24.5 g/100 g) and insoluble dietary fibre (64.1 g/100 g) [5]. The insoluble fibre-rich fraction comprising of insoluble dietary fibre, alcohol-insoluble solids, and water-insoluble solids (84.9-93.3 g/100 g) [5] becomes the predominant component in the (defatted) seed after oil extraction and these components are primarily made of cellulose, pectic substances, and hemicellulose [27,28]. Based on solubility, dietary fibre can be split into two groups: insoluble dietary fibre (IDF) and soluble dietary fibre (SDF).

Total dietary fibre (DF) is resistant to digestion and absorption in the human small intestine and can be partially fermented in the large intestine. Numerous studies have demonstrated that dietary fibre can minimise the likelihood of gastrointestinal disease, protect the gastrointestinal tract, and encourage healthy gut construction [28]. DF, depending on the source may bring changes in enzyme activity of some intestinal microflora, in the synthesis of metabolites, and in metabolic processes, which then affects intestinal function, health, and structure [4,6]. DFs physiological and chemical characteristics may help to explain how they work in food. DF-rich products and diets have grown in popularity as functional food ingredients for their health benefitting behaviour. This has inspired food researchers to hunt for new fibre sources and to develop high-fibre products [12]. A very little research has been done on the fibre present in passion fruit seeds.

The extraction procedure used is crucial for the use of plant bioactive components. DF has been extracted using a variety of techniques, including chemical, biological, and

physical methods [14,35], which may alter the effectiveness and quality of the extracted fibre [13]. Furthermore, several of these techniques have several disadvantages, such as prolonged reaction periods, larger solvent consumption, requirements of higher temperatures, and the introduction of many ions throughout the reaction process [16,35].

Having the advantages of high extraction efficiency, low energy consumption, and ease of use, ultrasonic-assisted extraction (UAE) has recently drawn increasing attention in comparison to thermal, enzymatic, and chemical treatments [13]. UAE can somewhat improve the physicochemical characteristics of DF, such as its capacity to hold water and oil, and swelling and rheological characteristics [21]. For higher extraction efficiency, alkaline treatment along with ultrasonication treatment has been used instead of the conventional alkaline treatment, which is known to take a longer time to extract the dietary fibres from different plant matrices [13,38]. Many reports have discussed the use of alkaline-UAE treatment in the extraction of fibres from different plant matrices, such as papaya peel [38], *Nannochloropsis oceanica* [13], and *Akebia trifoliata* (Thunb.) Koidz seeds [17]. However, no study has been found on the application of alkaline UAE treatment to extract DF from passion fruit defatted seed (DPFS) to date.

Alkaline extraction of fibre also involves chemical processing, such as acid neutralisation after alkaline treatment, which adds to the complexity and cost of the process. Again, chemically processed fibre cannot be integrated directly into the food system. According to Krishnaiah et al. [18], alkaline treatment has a negative effect on pectin as the C-O groups of hemicellulose and pectin decreased significantly with treatment. This may affect some functional properties of the extracted pectin like emulsification [11,31,39]. Therefore, it is necessary to extract DF using only ultrasonication process and compare it with other methods like alkaline-UAE and only alkaline extraction process. No investigation on the extraction of DF using ultrasonication procedure from defatted passion fruit seeds has yet been reported.

In this chapter, DF was extracted from DPFS using UAE and based on single-factor trials, extraction parameters were adjusted and optimized using a Box-Behnken design (BBD). The ultrasonication treatment (optimize conditioned) was compared with alkaline-UAE and only alkaline treatments for extraction of DF. The extracted DFs were analysed for physicochemical and functional properties, amylase inhibition, crystallinity, functional groups, morphology, and thermal properties. Since creating food emulsions is the primary goal of the extracted fibre, emulsion ability and cytotoxicity were also investigated.

5B.2. Materials and Methods

5B.2.1. Sample preparation

The passion fruits were obtained from Bishnupur district, Manipur, India. The defatted PFS fraction obtained (**Chapter 5A)** was used as the raw material for the present work. The defatted passion fruit seed (DPFS) fraction was stored in a plastic bag at -18 ℃ until further use. The standards used for HPLC were procured from Sigma and all other chemicals were of analytical grade. All the experiments were carried out in triplicates.

5B.2.2. Methods of extraction of total dietary fibres (DFs) from DPFS

5B.2.2.1. Alkaline extraction method of DFs

The traditional alkaline extraction method used by Ding et al. [13] was followed with a minor modification to extract the DF from DPFS waste. In a beaker, coarsely ground DPFS powder was mixed with 1 % NaOH to create a suspension with an optimal solid to liquid ratio (already optimized ratio). The suspension was mixed in a magnetic stirrer at 250 rpm at room temperature for 5 min, followed by stirring at 1000 rpm at 50 ℃ for 30 min, and neutralisation with HCl. Three volumes of ethanol were added to the mixture, and the mixture was kept undisturbed for 1 h to precipitate SDF. Finally, the whole solution (insoluble and soluble fibre) was centrifuged at 8000 rpm for 30 min and the collected precipitate was washed for three times and dried at 50 ℃ in a drier. The dried fibre was kept at refrigeration temperature in a desiccator until required. The obtained fibre was named as alkaline-treated dietary fibre and coded as ADF.

5B.2.2.2. Ultrasound-assisted alkaline extraction method of DFs

The ultrasonication aided alkaline extraction method used by Ding et al. [13] was modified slightly to extract DFs from DPFS powder. The extraction was performed using an ultrasonic probe (U500, Takashi, Japan). Accurate weight of coarsely ground DPFS was transferred to a beaker. Each extraction was carried out under carefully controlled ultrasonication, and 1 % NaOH solution was added to the beaker in accordance with the experimental design **(Table 5B.1).** The effects of extraction time (10–30 min), solid–liquid ratio (5–20 g/100 mL), and ultrasonic power (100–300 W) were evaluated at room temperature. Like alkaline extraction procedure, the treated fibre underwent precipitation, centrifugal separation, and drying. The total DF that was isolated was termed as ultrasound-assisted alkaline treated dietary fibre and coded as AUDF and was refrigerated for further examination.

5B.2.2.3. Ultrasound treatment of total dietary fibre

DPFS powder was added with the optimized ratio of the solid and-water (distilled water was used instead of alkaline water), which was already optimized in the alkaline ultrasound extraction process, and ultrasound was applied for up to 120 min at the optimised ultrasonication power, and the particle size and polydispersity index taken as responses were measured after every 30 min. The treatment period of 90 min was determined to be the optimum. Like alkaline extraction procedure, the treated fibre underwent precipitation, centrifugal separation, and drying process. The extracted fibre was named ultrasound extracted dietary fibre and coded as UDF and stored in a refrigerator for further analysis.

5B.2.3. Physicochemical properties of PFS and DPFS

Total ash, crude lipid, crude fibre, crude protein, and moisture content were determined according to standard methods [15,29] and the details are mentioned in **Chapter 5A**. The total dietary fibre, soluble dietary fibre, and insoluble dietary fibre were determined according to standard methods [13,35].

5B.2.4. Characterization of DFs

5B.2.4.1. Morphology of DFs

Surface morphology of ADF, AUDF and UDF was studied using a scanning electron microscope (SEM) (JSM 6390LV, JEOL, Japan), the details are mentioned in **Chapter 4.** 500X and 1500X magnifications were used for observation [3].

5B.2.4.2. Fourier transform-infrared spectroscopy (FTIR) of DFs

The absorbance infrared spectra of the ADF, AUDF, and UDF were recorded on an FTIR spectrophotometer (IMPACT 410, Nicolet, USA) as described by Choi et al. [8], the details of which are mentioned in **Chapter 4**.

5B.2.4.3. X-ray diffraction (XRD) of DFs

XRD was performed to evaluate the crystallinity of ADF, AUDF, and UDF using powder X-ray diffractometer (D8 FOCUS, Bruker Axs, Germany) [8] (details are mentioned in **Chapter 4)**.

Percentage of crystallinity was calculated using following equation **(Eq. 5B.1)**

$$\text{Reletive Crystallinity}(\%) = \frac{\text{Area of the crytalline area}}{\text{Total area}} \times 100 \qquad (5B.1)$$

5B.2.4.4. Thermogravimetric analysis (TGA) of DFs

Thermal stability of ADF, AUDF, and UDF was determined using a Thermo gravimetric analyser (TGA, Netzsch, Germany) [3] (details are mentioned in **Chapter 4**).

5B.2.5. Physicochemical properties of DFs

5B.2.5.1. Swelling capacity (SC), water holding capacity (WHC), and oil holding capacity (OHC)

SC, WHC, and OHC were measured according to the methods developed by Zhang et al. [38] with slight modification. Briefly, 75 mL of deionized water (V_1) was mixed with W_1 g of seed fibre, and the mixture was magnetically agitated for 24 h. Following the measurement of the suspension volume (V_2), the suspension was centrifuged for 10 min at a speed of 6000 rpm. The wet fibre's weight (W_2) was measured after the supernatant was drained away. The SC and WHC of the fibre were expressed by **Eq. 5B.2** and **Eq. 5B.3,** respectively, as follows:

$$\text{SC}\ \left(\frac{\text{mL}}{\text{g}}\right) = \frac{V_2 - V_1}{W_1} \quad (5B.2)$$

$$\text{WHC}\left(\frac{\text{g}}{\text{g}}\right) = \frac{W_2 - W_1}{W_1} \quad (5B.3)$$

The OHC of DFs was determined according to the method of Zhang et al. [38] with slight modification. Firstly, 20 mL of sunflower oil and W_1 g of DFs were mixed and magnetically stirred for 24 h. The weight of the fibre (W_2) was then measured after the suspension was centrifuged at 3000 rpm for 10 min. OHC was determined using **Eq. 5B.4.**

$$\text{OHC}\left(\frac{\text{g}}{\text{g}}\right) = \frac{W_2 - W_1}{W_1} \quad (5B.4)$$

5B.2.5.2. Cation-exchange capacity (CEC) of DFs

To determine the CEC, the method developed by Chau and Huang [5] was used with slight modification. Briefly, fibre samples were soaked in 0.1 mol/L HCl for 48 h and then filtered. The residue was collected and then freeze-dried. A few drops of phenolphthalein indicator and 5 g/100 mL NaCl solution of 100 mL were mixed with 0.2 g of the freeze-dried sample. The mixture was then progressively titrated against 0.1 mol/L of NaOH solution while being magnetically agitated. The volume of added NaOH solution was then measured. In place of HCl, distilled water was used to determine a blank sample.

The following equation **(Eq. 5B.5)** was used to determine the sample's CEC:

$$\text{CEC}\left(\frac{\text{mmol}}{\text{g}}\right) = \frac{V_2 - V_1}{C/M} \quad (5B.5)$$

where C, V_1 and V_2 is the concentration, titrated volume of NaOH for sample, and blank, respectively. M is the weight of DFs (g).

5B.2.5.3. Emulsifying capacity (EC) of DFs

Briefly, 5 g of DFs were dissolved in 10 mL of deionized water and homogenised using a high-speed homogenizer at 12400 rpm for 10 min with olive oil. The emulsions were centrifuged (1500 g, 5 min), and the tube's total height as well as the height of the emulsified layer were measured [1] using **Eq. 5B.6.**

$$\text{EC}(\%) = \frac{\text{Height of the emulsifying layer}}{\text{Height of total emulsion}} \quad (5B.6)$$

5B.2.6. Functional properties of DFs

5B.2.6.1. Glucose-adsorption capacity (GAC) and α-amylase inhibitory effect of DFs

The method used to assess the GAC (mmol glucose/g fibre) of the DFs was slightly modified from that provided by Chau and Huang [5]. In an experimental beaker, 100 mL of glucose solution (100 mmol/L) and 1 g of DFs were mixed and the final glucose content of the mixture was determined as per Ou et al. [26]. The method used by Chau and Huang [5] with slight modification was applied to measure the amylase inhibitory effect (%) of the DFs. After mixing 1 g of DFs with 4 mg of α-amylase in 40 ml of 4 % potato starch solution for 30 min, the mixture's ultimate glucose concentration was determined. The percentage difference between the control (without fibre) and treated groups in the rate of glucose production (mmol/h) was used to calculate the amylase inhibitory effect (%).

5B.2.6.2. Cytotoxicity assay of DFs

Cell culture: THP-1 cells were procured from ATCC (USA) and maintained in RPMI-1640 medium supplemented with 2 mM glutamine, 10% FBS and Penicillin-streptomycin (100 μg/mL) at 37 °C and 5% CO_2 atmosphere.

Assay: THP-1 cells (5×10^3 cells/well) were treated with 150 nM phorbol 12-myristate 13-acetate (PMA) for 48 h in a 96-well plate and allowed for differentiation to macrophages [10]. Cells were washed with PBS, followed by the addition of 10 % FBS-containing media. After 24 h of the resting phase, cells were treated with increasing concentration of the extract in 1 % RPMI-1640 containing medium in triplicates for 24 h

in CO_2 incubator. Following incubation, cells were quantified with MTT at 590 nm wavelength using UV-Visible spectrophotometer (Multiscan Go, Thermo Scientific, Waltham, MA, USA) [33].

5B.2.7. Experimental design of alkaline-ultrasonic extraction

In this study, experiments were designed using the response surface methodology. For the alkaline-ultrasonic extraction method, three independent parameters namely treatment time (A), ultrasonic power (B), and solid to liquid ratio (C) were selected to determine the yield of fibre taken as the response.

According to Box-Behnken Design (BBD), 17 experimental runs were performed, including five runs at the zero experiment. According to **Eq. 5B.7**, the independent variables listed in **Table 5B.1** were coded.

$$x_i = \frac{X_i - X_{i0}}{\Delta X_i} \quad (5B.7)$$

Where, X_i and x_i are the actual and coded vales of the 'i' independent variable, X_{i0} is actual value of the 'i' independent variable at the central point, and ΔX_i is the step change of the dimensionless value. BBD design for the extraction was fitted to a second-order quadratic model. Design-Expert Version 7.1.2 (Stat-Ease, Inc. MN) was used for designing the experiment.

Table 5B.1. Real and coded values of the variables.

Experimental Variables	Code	Coded levels		
		-1	0	+1
Treatment Time (Min)	X_1	10	20	30
Ultrasonic Power (Watt)	X_2	100	200	300
Solid to liquid ratio (g/100 mL)	X_3	5	12.5	20

5B.2.8. Optimization

Based on higher desirability value optimization was performed as in **Chapter 3**.

5B.2.9. Statistical Analysis

The data were statistically analyzed using IBM SPSS statistical software (version 21.0, SPSS Inc., Chicago, IL, USA). Design-Expert Version 7.1.2 (Stat-Ease, Inc. MN) was used for analysing the experimental data.

5B.3. Results and Discussion

5B.3.1. Physicochemical properties of PFS and DFPS

The seed content in fresh passion fruit was 16.5 g/100 g. **Table 5B.2** gives the composition of the raw PFS and DFPS. The raw seed had high levels of crude fat (24.4 g/100 g) and crude fibre (51.6 g/100 g), but low levels of crude protein (11.6 g/100 g), ash (1.6 g/100 g), and carbohydrate (1.2 g/100 g) **(Table 5B.2)**. The total dietary fibre content (DFs) in the fresh PFS was 34.1 g/100 g, which constitutes approximately 66 % of crude fibre. The DFs content was significantly raised in defatted seed, reaching 55.8 g/100 g. The most prevalent fibre fraction (52.2 g/100 g) in defatted seed was discovered to be IDF, which constituted 95.5 % of the total dietary fibre present. Similar results were reported by Chau and Huang [5], who reported 84.9 g/100 g IDF in PFS.

Table 5B.2. Physicochemical composition of the raw and defatted passion fruit seed.

Parameters	Amount	
	Raw seed	**Defatted seed**
Moisture content (g/100 g)	9.6±0.6	3.2±0.5
Total lipids (g/100 g)	24.4 ±1.8	0.6±0.2
Crude fibre (g/100 g)	51.6±1.8	76.5±1.2
Crude protein (g/100 g)	11.6±0.9	16.3±0.6
Ash (g/100 g)	1.6±0.2	1.9±0.18
Carbohydrates (g/100 g)	1.2±0.6	1.5±0.4
Total dietary fibre (g/100 g)	34.1±1.9	55.8±2.1
Insoluble dietary fibre (g/100 g)	32.4±1.1	52.2±1.1
Soluble dietary fibre (g/100 g)	1.7±0.4	3.6±0.6

DPFS being a rich source of insoluble fibre, may exhibit advantageous physiological effects and favourable intestinal peristalsis due to an increase in faecal volume and a decrease in transit time [5]. According to Lopez-Vargas et al. [22], 90 % w/w of DF present in DPFS was IDF, which comprised of cellulose (41.43 %), hemicellulose (37.71 %), and lignin (16.80 %) and total dietary fiber content in a mixture of passion fruit seeds and pulp was 53.51 g/100 g. Chau et al. [5] observed cellulose, hemicellulose, and pectic substances as the major insoluble fibre fractions.

5B.3.2. Optimization of UAE-alkaline extraction of DFs

A single-factor experiment was run as the dependent index to determine the initial range of the independent parameters for the extraction process (**Table 5B.1**) and

response surface method was used to optimise the extraction conditions. The extraction yield of DFs from DPFS was used as an assessment index.

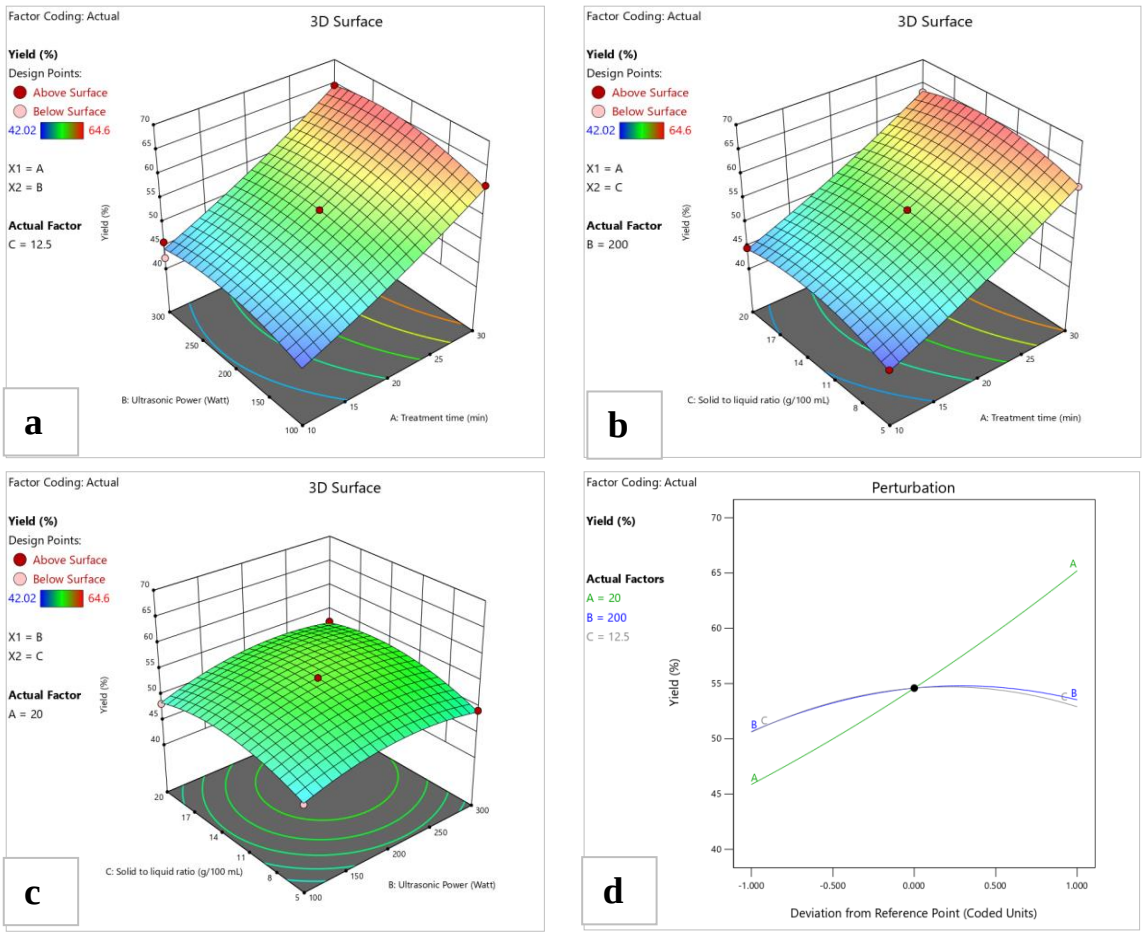

Fig. 5B.1. Extraction yield of dietary fibre from defatted passion fruit seed as effected by: (a) Time and power; (b) Time and solid-liquid; (c) Solid-liquid ratio and power ratio, and (d) Perturbation (deviation from reference point).

The extraction yield of DF grew to its highest as the time was extended from 10 min to 30 min, as shown in **Fig. 5B.1a** and **1b,** while other parameters were held constant. This suggested that a longer UAE time may decrease the particle size of extracted DF and enhance mass transfer rate. Additionally, extending the treatment period improved the extraction yield because it absorbed more energy. This behaviour was in concurrence with Chen et al. [7], who noted that treatment time of up to 40 min enhanced the extraction yield of soluble and insoluble DF.

Similar to this, the extraction yield steadily increased as the ultrasonication power was increased from 100 to 300 W (**Fig. 5B.1a** and **1c),** while other parameters were kept constant. Increasing power, it is suggested, may result in smaller particles and a greater surface area, hastening the mass transfer of intracellular materials. Excessive high power

may cause the degradation of DFs which may not precipitate during centrifugation. Therefore, 284.8 W was taken as the ideal amplitude. According to **Fig. 5B.1b** and **1c,** the extraction yield increased to about 10 g/100 mL before a decreasing trend was noticed. Similar patterns were documented by Chen et al. [7] as well. **Fig. 5B.1d** depicts the Perturbation (deviation from reference).

Table 5B.3. ANOVA table for yield of DFs extraction using ultrasonication.

Source	Sum of Squares	dF	Mean Square	F-value	p-value	
Model	805.14	9	89.46	90.49	< 0.0001	Significant
A −Treatment time	523.50	1	523.50	529.53	< 0.0001	
B −Ultrasonic Power	11.64	1	11.64	11.77	0.0110	
C −Solid to liquid ratio	10.58	1	10.58	10.70	0.0136	
AB	0.4306	1	0.4306	0.4356	0.5304	
AC	0.0576	1	0.0576	0.0583	0.8162	
BC	0.7056	1	0.7056	0.7137	0.4261	
A^2	3.11	1	3.11	3.15	0.1194	
B^2	21.45	1	21.45	21.70	0.0023	
C^2	27.54	1	27.54	27.86	0.0012	
Residual	6.92	7	0.9886			
Lack of Fit	0.8650	2	0.4325	0.3571	0.7162	Not significant
Pure Error	6.06	5	1.21			
Cor Total	812.06	16				

To optimise the conditions for alkaline-UAE extraction, 17 experiments were carried out using a BBD design of RSM. Regression analysis was used to evaluate the experimental findings and test for significance **(Table 5B.3).** The quadratic regression at **Eq. 5B.8** explains the extraction yield.

$$\text{Yield}=54.59+9.67\times A+1.44\times B+1.15\times C+0.45\times AB+0.12\times AC+0.42\times BC+0.95\times A^2-2.50\times B^2-2.83\times C^2 \quad (5B.8)$$

where, A, B and C are the coded values.

The ANOVA analysis in **Table 5B.3** helps to assess and filter the effects of the important factors in linear and quadratic forms. The F-value and P-value of the

developed quadratic model were 90.49 and <0.0001, respectively. Generally, higher F-values and lower p-values ($p<0.05$) indicate that the corresponding variables are more significant [38]. In addition, the ANOVA regression model ($p<0.01$), the R^2 (0.9915) and coefficient of variation CV % (1.89) proved the significant importance of the quadratic model for predicting the extraction yield of DF. The non-significant ($p=0.7162>0.05$) value for lack-of-fit demonstrated that the quadratic model can successfully forecast the yield of DFs. In this case, A, B, C, B^2 and C^2 were shown to be significant model terms. The other coefficients were insignificant ($p>0.05$). The lack-of-fit was not significant relative to the pure error because the corresponding F-value was 0.3571. In summary, the optimum conditions for the ultrasound-assisted alkali extraction of DF from DPFS were as follows: solid to liquid ratio of 8.23, ultrasound power of 284.8 W, ultrasound time of 28.3 min, and under these conditions, the production of DF was 61.35 % of total fibre. The yield of ADF, AUDF, and UDF was found to be 52.8 %, 61.35 % and 50.4 %, respectively. For the practical applicability, experimental conditions taken were solid to liquid ratio of 8.3, ultrasound power of 285 W, and ultrasound time of 28.5 min.

5B.3.3. Characterization of ADF, AUDF, and UDF

5B.3.3.1. SEM analysis of DFs

The microstructure of ADF, AUDF, and UDF fibres that were extracted using various extraction procedures are shown in **Fig. 5B.2**. The seed fibre in the ADF was in a lump with a smooth surface and a tight texture or compact structure, as illustrated in **Fig. 5B**.**2a** and **2b.** This may be due to molecular interactions that made the fibre surface smooth and continuous [38]. **Fig. 5B.2c** and **2d** depicts the microstructure of AUDF fibre. AUDFs had flaky structures that were roughly stacked together. This is because alkali and ultrasound induces cell tissue to deform and the cellulose packing in the cell wall to dissolve [38]. The cross-linking between polysaccharide molecules is destroyed by prolonged ultrasonic treatment [21,38], because of which the UDFs were destroyed at the cellular level and changed to a spherical shape with a significantly decreased size (nano size range) range when ultrasonic power used was noticeably high **(Fig. 5B.2e** and **2f).** Additionally, as the structure of the fibre changes, so does its usefulness as nano food ingredient with better functional properties [21].

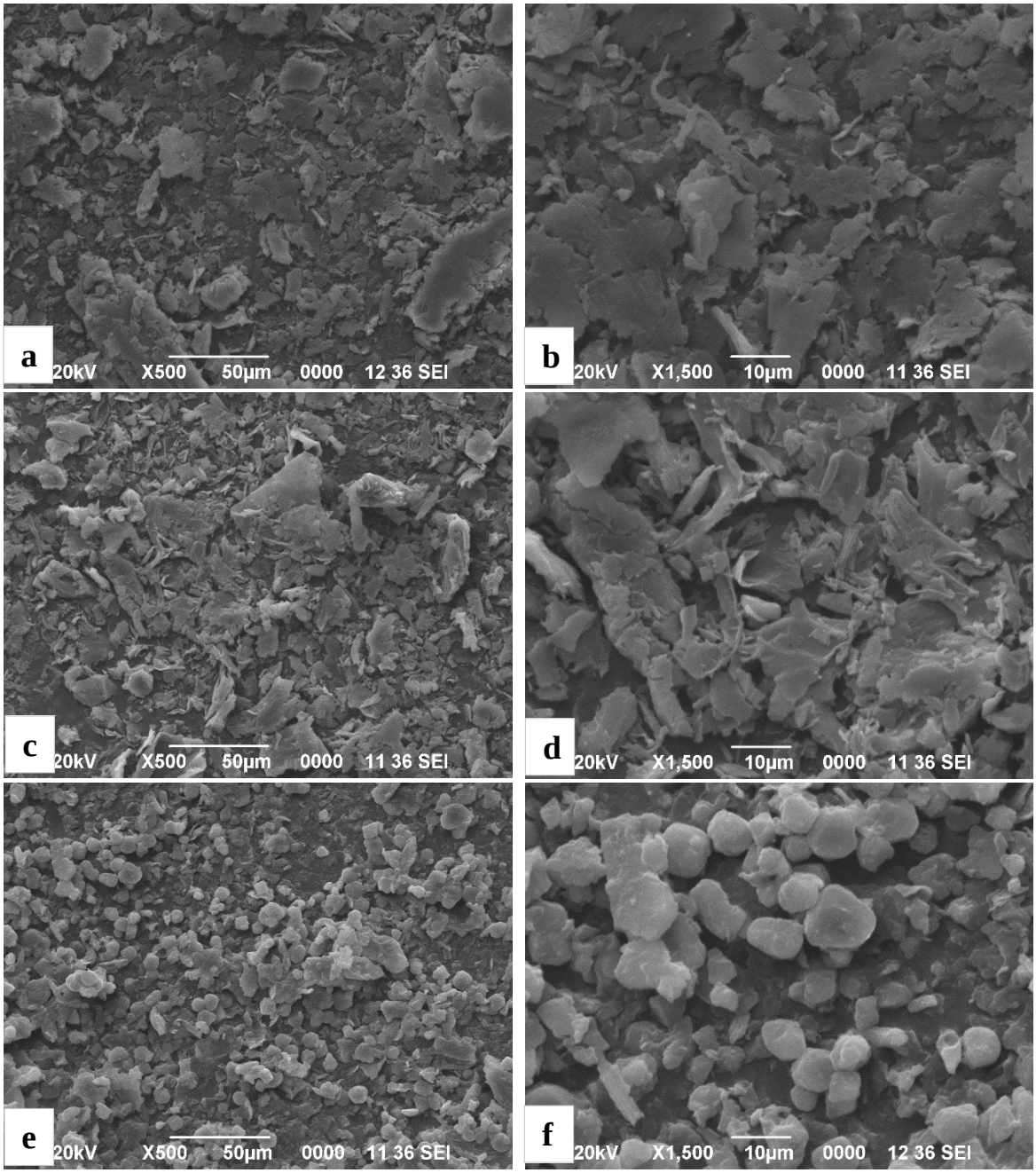

Fig. 5B.2. SEM analysis of (a) ADF(500X), (b) ADF(1500X), (c) AUDF(500X), (d) AUDF(1500X), (e) UDF(500X) and (f) UDF(1500X) sample.

5.3.3.2. FT-IR spectra of DFs

Through FTIR analysis, the chemical composition, and the functional groups of ADF, UDF, and AUDF were determined. **Table 5B.4** lists the functional groups of cellulose, hemicellulose, pectin, and lignin that are present in these DFs along with their corresponding IR spectra [18,38]. After subjecting the fibre constituents to surface treatments, the FTIR spectrum can be used to study the shifted functional groups of DFs [38].

Table 5B.4. FTIR transmittance peaks of the constituents of passion fruit seed fibres.

Wavenumbers (cm^{-1})	**Functional groups**	**Possible assignment**
3431	-OH stretching vibrations	Cellulose, hemicellulose, and lignin
2916, 2856	C-H stretching vibrations	Lignin, hemicellulose, and cellulose
1742	C=O stretching vibrations	Carboxyl groups of hemicellulose and pectin
1636	-OH bending mode	Presence of water in hemicellulose
1421	CH_2 stretching	Cellulose
1261	C-O stretching	Acetyl groups of lignin
1060	C-O stretching	Lignin and cellulose

As shown in **Fig. 5B.3**, mainly eight peaks, with positions at 1060, 1261, 1421, 1636, 1742, 2856, 2916, and 3431cm^{-1} emerged. The stretching vibrations of hydroxyl groups (-OH) of fibres (possibly cellulose, and hemicellulose and lignin) are responsible for the

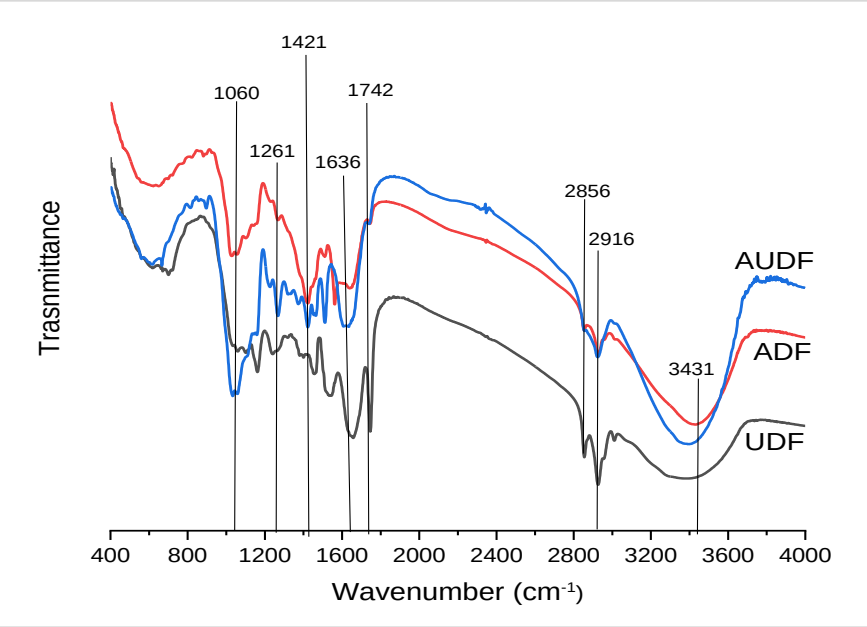

Fig. 5B.3. FTIR analysis of ADF, AUDF, and UDF.

large peaks at 3431 cm^{-1}, and the intensity of -OH stretching vibrations decreased after the prolonged US treatment for UDF fibre. The band at 2916 cm^{-1}, which in the ADF and AUDF indicates the C-H stretching of lignin, slightly changed to 2930 cm^{-1}, possibly due to the elimination of lignin after ultrasonic treatment [18]. The band in the UDFs at 1742 cm^{-1} denotes the C-O groups of pectin and hemicellulose, which substantially decreased with alkali treatment. This confirmed that ultrasound process

alone was ineffective in removing pectin and hemicellulose from the surface of the fibres [18]. On the other hand, alkali treatment alone caused a considerable drop in the peak at 1261 cm^{-1} that corresponds to the C=O stretching of lignin's acetyl groups.

From these findings, it can be concluded that alkali, as well as the combination treatment of alkali and ultrasound, can remove the functional groups of fibres specially hemicellulose, pectin, and lignin from the surface of passion fruit seed fibre. This study demonstrated that ultrasonic treatment alone had no appreciable effects on the removal of hemicellulose and pectin. However, alkali treatment alone was found to have a positive effect on removing amorphous materials from the surface of DFs, such as hemicellulose, lignin, and pectin [7,18]. Similar observations were reported on the preparation of dietary fibre from papaya peel [38] and sisal fibres [18].

5.3.3.3. XRD of DFs

As shown in **Fig. 5B.4,** the XRD patterns were used to investigate the effects of different extraction techniques on the crystal structure of DFs obtained from DPFS. In this investigation, defatted seed fibre comprised of cellulose (41.43%), hemicellulos (37.71%), and lignin (16.80%). The passion fruit seed fibres are made up of crystalline and amorphous (non-crystalline) regions, with the non-crystalline portion primarily containing hemicellulose, pectin and lignin [16,21].

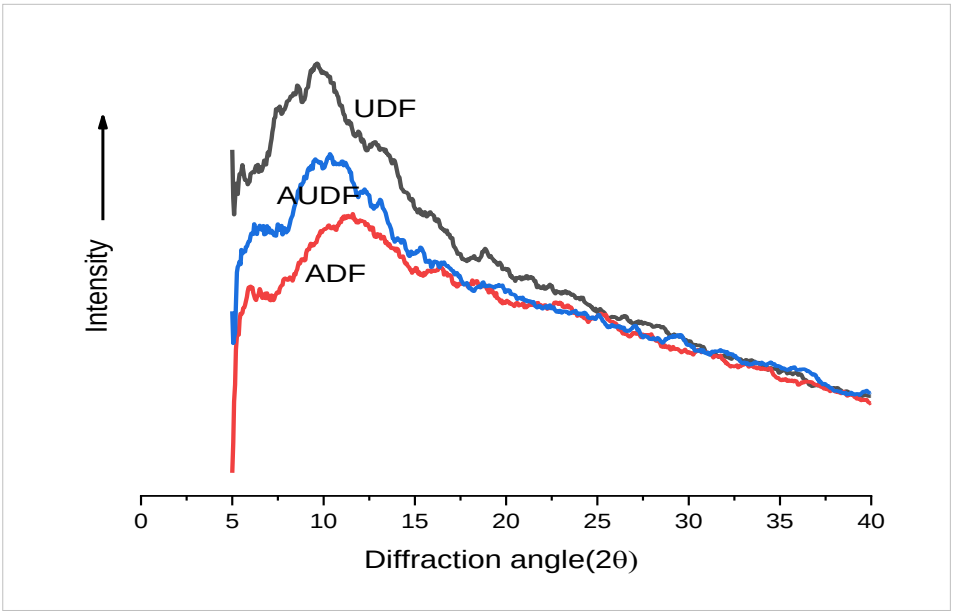

Fig. 5B.4. XRD graphs of ADF, AUDF, and UDF

All the extracted dietary fibre samples showed a similar trend. DPFS showed prominent characteristic diffraction peaks at approximately 10° with minor peaks at 8.5°.

Maximum relative crystallinity of 31.6 % was seen for ADF and minimum of 18.4 % in AUDF **(Table 5B.5**). The relative crystalline cellulose phase of DFs gives a sharp peak with high intensity [18]. The cellulose in the DFs on alkali treatment becomes alkaline cellulose and its formation depends on alkali concentration and treatment conditions. The two forms of alkali-treated cellulose that are most frequently found are Na+-cellulose I and Na+-cellulose II. According to Nishiyama et al. [25], the alkali treatment causes the cellulose molecules in their amorphous form to rearrange themselves into crystalline phase. Krishnaiah et al. [18] also observed similar results in sisal fibres at a higher concentration of alkali.

Table 5B.5. Relative crystallinity and physicochemical and functional properties of DFs

Parameters	**ADF**	**AUDF**	**UDF**
Relative crystallinity (%)	31.6±0.4	18.4±0.6	22.8±0.2
Bulk density (g/mL)	0.5±0.04	0.7±0.05	0.6±0.05
Water holding capacity (mL/g)	2.2±0.09	3.1±0.07	2.9±0.06
Oil holding capacity (g/g)	3.4±0.05	3.9±0.6	4.1±0.5
Swelling capacity (mL/g)	7.5±0.09	11.4±0.08	15.7±0.08
Cation exchange capacity (meq/kg)	54.3±0.7	73.5±0.6	53.2±0.7
Emulsion capacity (%)	38.9±0.4	44.6±0.7	50.1±0.07
Glucose-adsorption capacity (mmol glucose/g fibre)	9.5±0.09	16.7±0.1	18.3±0.01
Amylase inhibitory effect (%)	29.4±0.4	33.5±0.5	32.3±0.07

Ultrasonication treatment decreased the crystallinity indicating the severe but not complete damage of the crystal structure of DF by ultrasound, making it more amorphous. Additionally, the interaction between the DF molecules weakens and this facilitates solubility, swelling, and water- and oil-holding capabilities of DF. Ultrasonication, in addition, lowers the degree of polymerization [38]. As already discussed for FTIR results, the band appearing in UDFs at 1742 cm^{-1} is indicative of C-O groups of hemicellulose and pectin and these groups decreased significantly with alkali treatment **(Fig. 5B.3).** This reduction in hemicellulose and pectin is mainly responsible for the loss of semicrystalline structure. For AUDF, the lowest relative crystallinity was observed, which may be due to the combined effect of ultrasound and alkaline treatment. Zhang et al. [38] observed lower crystallinity for combined ultrasonic and alkaline treatment as compared to conventional alkaline extraction. Thus, alkali

treatment is effective and useful to remove the amorphous materials and hence, to improve the mechanical and thermal properties [18].

5.3.3.4. TGA analysis of DFs

One of the crucial factors during the thermal processing of food unit operations is the thermal stability of a polymer. To assess the changes in the thermal properties and thermal stability of ADF, AUDF, and UDF, TGA was carried out in the 0-900 ℃ temperature range **(Fig. 5B.5)**. Results showed significant changes in DFs at different temperature ranges (40–235 ℃, 235–440 ℃, and 440-900 ℃) and DF was observed to have different degradation kinetics at these temperature ranges.

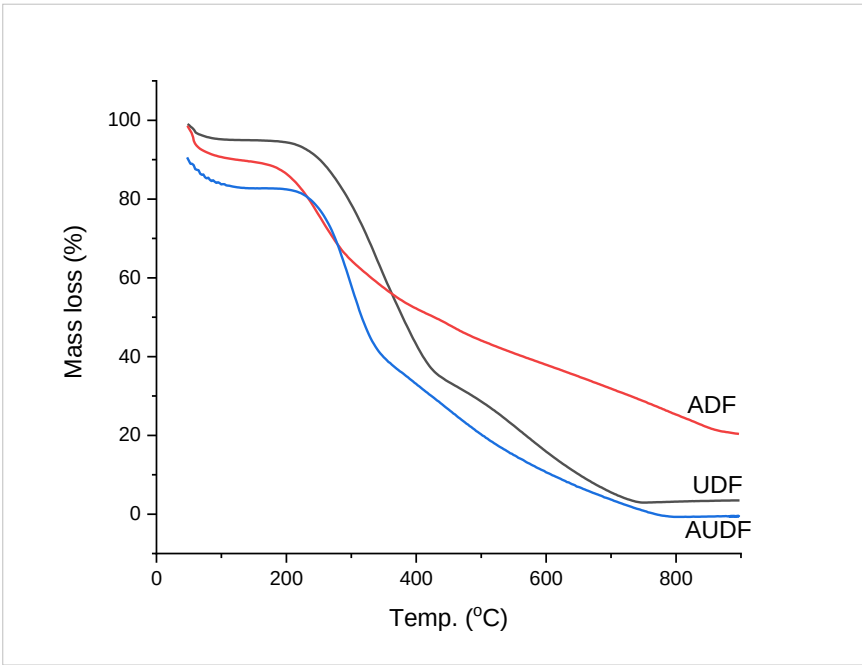

Fig. 5B.5. TGA analysis of ADF, AUDF and UDF.

ADF was observed to have temperature degradation at 35–104 ℃, 104–203 ℃, 203–285 ℃, and further up to 900 ℃. Moriana et al. [24] observed the first temperature range to occur from 40–200 ℃, which was explained to be due to the evaporation of absorbed water. The evaporation of humidity from the materials or the low molecular weight molecules left over from the isolation methods caused a modest weight loss in each case, which was detected at temperatures between 25 and 150 ℃ [7].

Studies have shown that cellulose begins to pyrolyze at 315 ℃ and this continues up to 440 ℃, while hemicellulose degrades rapidly between 210 and 350 ℃ [24]. Due to the presence of different functional groups in cellulose, hemicellulose, and lignin that are present in DFs, variable thermal breakdown temperatures were observed. The weight

loss of ADF was less than AUDF and UDF, indicating that ADF had greater thermal stability than AUDF and UDF. The thermal stability order was ADF>UDF>AUDF. This observation strongly indicated that moisture loss was maximum after alkali treatment, which is due to the removal of amorphous materials, as was also confirmed by the maximum crystallinity of ADF **(Fig. 5B.4).** Also, removal of surface impurities i.e. wax and oil that makes the fibre surface clean also enhances the thermal stability of fibres [18]. As ultrasound was not able to remove the pectin, rapid thermal degradation occurred at a later stage in UDF.

5.3.4. Physicochemical properties of extracted dietary fibre

WHC is a material's capacity to hold water under the influence of external centrifugal gravity or compression. Physically imprisoned water, which makes up the majority of this capacity, is combined with linked water, and hydrodynamic water. WHC formation is also based on the hydrophilic group and reticular structure of the DFs [20]. As shown in **Table 5B.5**, ADF, AUDF, and UDF had WHC of 2.2, 3.1, and 2.9 mL/g of DPFS. WHC values suggested that DF may be used in products that call for hydration, viscosity development, and freshness preservation, such as baked goods or items made from cooked meat [22].

In UDF, the WHC had increased, which may be due to the shift from high order to less ordered crystal structure and to structural loss of DFs [38]. Again, after ultrasonication treatment, owing to smaller particle size and resultant larger specific surface area, the WHC was high [20]. But alkali treatment decreased the hemicellulose, lignin, and pectin, which is responsible for the semicrystalline structure, as was confirmed by FTIR analysis [18] and as a result the increased crystallinity ultimately caused reduction in WHC [25]. A greater WHC is preferable since it means the food can retain more moisture and experience less dehydration-related shrinking. Furthermore, WHC is a crucial component of DF from physiological and technological standpoints [5].

Plant polysaccharides have a chemical structure that is related to OHC, which is a technical attribute that depends on surface characteristics, particle size distribution, overall charge density, thickness, and the hydrophobicity of the fibre particle [20]. OHC values for ADF, AUDF, and UDF were 3.4 g/g, 3.9 g/g, and 4.1 g/g, respectively **(Table 5B.5)**. The fibre that had been ultrasonically treated had the highest OHC capacity. A higher OHC indicates superior sensory qualities, longer shelf life, and increased stability

of high-fat foods like cookies [20]. In comparison to other derived fibres, such as rice bran dietary fibre (4.58–4.64 g/g) [20] and coconut fibre (4.68 g/g) [14], OHC value of passion fruit seed fibre is lower. According to López-Vargas et al. [22], the mixture of pulp and seeds powder of yellow passion fruit mixture had 1.80 g/g of water-holding capacity and 1.43 g/g of oil-holding capacity, while Chau and Huang [5] reported the water-holding capacity (ml/g) and oil-holding capacity (g/g) for passion fruit seed fibre to be in the range of 2.37-3.20 and 2.07-3.72 (g/g), respectively.

ADF, AUDF, and UDF had a cation-exchange capacity (meq/kg) of 54.3, 73.5, and 53.2, respectively **(Table 5B.5)**. According to Lopez-Vargas et al. [22], fibres with a higher cation-exchange capacity have the potential to trap, disrupt, and disintegrate the lipid emulsion, which would reduce the diffusion and absorption of lipids and cholesterol in the small intestine [5].

The emulsion capacity (EC) of ADF, AUDF and UDF was 38.9 %, 44.6 % and 50.1 %, respectively **(Table 5B.5)**. The EC value of UDF was almost at a critical limit of a good emulsifier. The higher EC value in UDF was because ultrasonication had retained hemicellulose, and pectin to a great extent [18], and the better emulsification properties of pectin is already well established [11]. As alkaline treatment removed these fractions **(Fig. 5B.3),** the EC of ADF was the lowest. The higher protein content [32,34,36] and pectin content [11] of DFs may be the cause of higher EC. Pectin conjugation with protein isolate through physical treatment also significantly improves emusification properties [19,23]. SDF that was extracted from papaya peel by Zhang et al. [38] using an ultrasound-assisted alkali extraction technique exhibited high degree of thermal stability, WHC, and OHC.

5.3.5. Functional properties of extracted DFs

5.3.5.1. The glucose-adsorption capacity (GAC) and α-amylase activity

The GAC of ADF, AUDF, and UDF was found to be 9.5 mmol glucose/g fibre, 16.7 mmol glucose/g fibre and 18.3 mmol glucose/g fibre, respectively **(Table 5B.5)**. Chau and Huang [5] reported similar outcomes. The increasing number of holes or gaps on the surface of the dietary fibre after ultrasonication significantly increased the GAC of passion fruit seed DFs. A greater GAC can be achieved by increasing the amount of glucose molecules trapped inside the fibre network after increasing the porosity and specific surface area of dietary fibre [40]. The crucial factors in DF capacity are to adsorb lipophilic substances and bind with glucose. The stronger ability to bind glucose

might be beneficial in lowering the concentration of available glucose in the small intestine [5].

Additionally, it was also observed that the DFs had a higher impact in lowering amylase activity (29.4-32.5 %) **(Table 5B.5)**. This in-vitro investigation showed that DFs could more effectively slow the rate of glucose synthesis (mmol/h) than cellulose. Additionally, it was discovered that the insoluble passion fruit seed fibre had a noticeably higher impact on lowering amylase activity (21.8-27.9 %). This finding suggested that the DFs' apparent effects on glucose absorption and amylase inhibition may work together to reduce the rate of absorption of glucose and the level of postprandial blood glucose.

5B.3.5.2. Cytotoxicity MTTS assay

Cytotoxicity studies are beneficial for identifying baseline cytotoxic processes shared by a variety of cells, but not for identifying toxins that are specific to an organ [37].

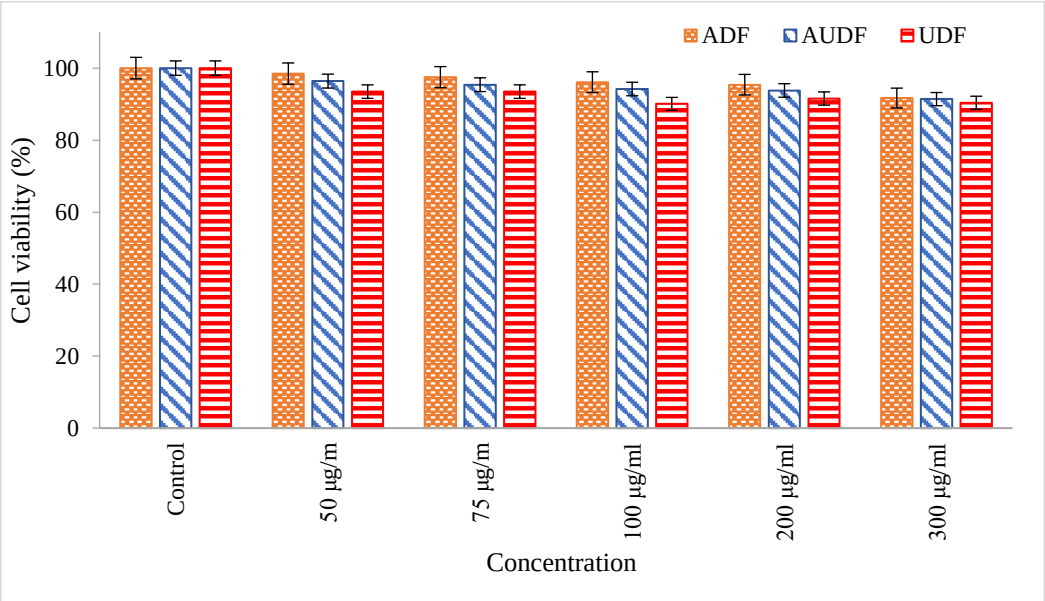

Fig. 5B.6. Cytotoxicity assay (MTT) of ADF, AUDF, and UDF.

To evaluate the cytotoxicity of ADF, AUDF, and UDF samples, THP-1 macrophage were treated with increasing concentration of the samples in triplicates. As shown in **Fig. 5B.6**, with an increase in concentration, there was a minor effect of the DFs on cell viability. Maximum cell death (9.6 %) was observed for UDF at 300 µg/mL concentration. For all samples, within the studied concentration, the cell viability values were higher than 90 %, which implied that all the samples are consumable and had

negligible toxicity. The acute toxicity studied by Am et al. [2] of passion fruit seed extract revealed that the extract was safe up to 5000 mg/kg, and they also made an observation that 3000 mg/kg was safe for 28 days from their results of sub chronic toxicity study.

5B.4. Conclusion

This study revealed that the edible passion fruit seed was rich in insoluble dietary fibre, which was mainly composed of cellulose, hemicellulose, lignin, and pectic substances. Alkaline, ultrasonic-alkaline, and ultrasonication extraction methods resulted in fibres with varying properties and behaviours. Even though ultrasonication treatment demonstrated better functional qualities, the yield was the lowest. Aside from the cation ion exchange capacity, all other parameters of the ultrasound treated DPFS, including WHC, OHC, SC, EC, glucose absorption capacity, and amylase inhibition activity increased. Since the method used to treat this agricultural by-product may affect how well the food fibres operate, there are distinctions between the dietary fibres extracted by alkaline, ultrasonication, and combined alkaline and ultrasonication treatments and these properties should be taken into consideration while selecting the extraction method. Insoluble fibre, which makes up 77.5 % of the total DF in DPFS, can be employed as a low-calorie bulk ingredient for fibre enrichment and in dietetic snacks. Since a considerable amount of these fibre rich passion fruit seeds are produced as a by-product of juice processing, they can be used as a valuable source of dietary fibre. More research into the physiological roles played by these insoluble DPFS fibres using animal feeding studies can be undertaken.

Bibliography

[1] Abdul-Hamid, A. and Luan, Y. S. Functional properties of dietary fibre prepared from defatted rice bran. *Food Chemistry*, 68(1):15–19, 2000.

[2] AM, A., Wasagyu, R., Lawal, M., Sahabi, A. and Zaharadeen, A. Acute and Subchronic Toxicity Study of Methanol Seed Extract of Passion Fruit (*Passiflora edulis var. flavicarpa*) in Albino Rats. *Food Science and quality management*, 56: 2016.

[3] Apostolidis, E. and Mandala, I. Modification of resistant starch nanoparticles using high-pressure homogenization treatment. *Food Hydrocolloids*, 103:105677, 2020.

[4] Barber, T. M., Kabisch, S., Pfeiffer, A. F. H. and Weickert, M. O. The health benefits of dietary fibre. *Nutrients*, 12(10):1–17, 2020.

[5] Chau, C. F. and Huang, Y. L. Characterization of passion fruit seed fibres — a potential fibre source. *Food Chemistry*, 85:189–194, 2004.

[6] Chau, C. F., Huang, Y. L. and Chang, F. Y. Effects of fibre derived from passion fruit seed on the activities of ileum mucosal enzymes and colonic bacterial enzymes in hamsters. *Journal of the Science of Food and Agriculture*, 85(12):2119–2124, 2005.

[7] Chen, W. et al. Individualization of cellulose nanofibers from wood using high-intensity ultrasonication combined with chemical pretreatments. *Carbohydrate Polymers*, 83(4):1804–1811, 2011.

[8] Choi, H. D. et al. Starch nanoparticles produced via acidic dry heat treatment as a stabilizer for a Pickering emulsion: Influence of the physical properties of particles. *Carbohydrate Polymers*, 239:116241, 2020.

[9] Corrêa, R. C. G. et al. The past decade findings related with nutritional composition, bioactive molecules and biotechnological applications of *Passiflora spp*. (passion fruit). *Trends in Food Science and Technology*, 58:79–95, 2016.

[10] Deka, A., Sharma, M., Sharma, M., Mukhopadhyay, R. and Doley, R. Purification and partial characterization of an anticoagulant PLA2 from the venom of Indian Daboia russelii that induces inflammation through upregulation of proinflammatory mediators. *Journal of Biochemical and Molecular Toxicology*, 31(10): 2017.

[11] Deng, Z. et al. Effects of cultivar and growth region on the structural, emulsifying and rheological characteristic of mango peel pectin. *Food Hydrocolloids*, 103:105707, 2020.

[12] Dhingra, D., Michael, M., Rajput, H. and Patil, R. T. Dietary fibre in foods: A review. *Journal of Food Science and Technology*, 49(3):255–266, 2012.

[13] Ding, Q. et al. Physicochemical and functional properties of dietary fiber from Nannochloropsis oceanica: A comparison of alkaline and ultrasonic-assisted alkaline extractions. *LWT- Food Science and Technolog*, 133:110080, 2020.

[14] Du, X. et al. Effects of different extraction methods on structure and properties of soluble dietary fiber from defatted coconut flour. *LWT- Food Science and Technology*, 143 111031, 2021.

[15] Firestone, D. *Official methods and recommended practices of the AOCS*.

American Oil Chemists' Society, 2009.

[16] Jaiswal, D., Devnani, G. L., Rajeshkumar, G., Sanjay, M. R. and Siengchin, S. Review on extraction, characterization, surface treatment and thermal degradation analysis of new cellulosic fibers as sustainable reinforcement in polymer composites. *Current Research in Green and Sustainable Chemistry*, 5: 2022.

[17] Jiang, Y. et al. Structure, physicochemical and bioactive properties of dietary fibers from *Akebia trifoliata* (Thunb.) Koidz. seeds using ultrasonication/shear emulsifying/microwave-assisted enzymatic extraction. *Food Research International*, 136: 2020.

[18] Krishnaiah, P., Ratnam, C. T. and Manickam, S. Enhancements in crystallinity, thermal stability, tensile modulus and strength of sisal fibres and their PP composites induced by the synergistic effects of alkali and high intensity ultrasound (HIU) treatments. *Ultrasonics Sonochemistry*, 34 729–742, 2017.

[19] Li, W. et al. Pickering emulsions stabilized by zein-proanthocyanidins-pectin ternary composites (ZPAAPs): Construction and delivery studies. *Food Chemistry*, 404:134642, 2023.

[20] Liu, Y., Zhang, H., Yi, C., Quan, K. and Lin, B. Chemical composition, structure, physicochemical and functional properties of rice bran dietary fiber modified by cellulase treatment. *Food Chemistry*, 342:128352, 2021.

[21] Liu, Y. et al. Effects of ultrasonic treatment and homogenization on physicochemical properties of okara dietary fibers for 3D printing cookies. *Ultrasonics Sonochemistry*, 77:105693, 2021.

[22] López-Vargas, J. H., Fernández-López, J., Pérez-Álvarez, J. A. and Viuda-Martos, M. Chemical, Physico-chemical, Technological, Antibacterial and antioxidant properties of dietary fiber powder obtained from yellow passion fruit (*Passiflora edulis var. flavicarpa*) co-products. *Food Research International*, 51(2):756–763, 2013.

[23] Ma, X. et al. Comparison of citrus pectin and apple pectin in conjugation with soy protein isolate (SPI) under controlled dry-heating conditions. *Food Chemistry*, 309:125501, 2020.

[24] Moriana, R., Vilaplana, F., Karlsson, S. and Ribes-Greus, A. Improved thermo-mechanical properties by the addition of natural fibres in starch-based sustainable biocomposites. *Composites Part A: Applied Science and Manufacturing*, 42(1):30–40, 2011.

[25] Nishiyama, Y., Kuga, S. and Okano, T. Mechanism of mercerization revealed by X-ray diffraction. *Journal of Wood Science*, 46(6):452–457, 2000.

[26] Ou, S., Kwok, K. C., Li, Y. and Fu, L. In vitro study of possible role of dietary fiber in lowering postprandial serum glucose. *Journal of Agricultural and Food Chemistry*, 49(2):1026–1029, 2001.

[27] Pereira, M. G., Hamerski, F., Andrade, E. F., Scheer, A. de P. and Corazza, M. L. Assessment of subcritical propane, ultrasound-assisted and Soxhlet extraction of oil from sweet passion fruit (*Passiflora alata Curtis*) seeds. *Journal of Supercritical Fluids*, 128:338–348, 2017.

[28] Qi, X. and Tester, R. F. Utilisation of dietary fibre (non-starch polysaccharide and resistant starch) molecules for diarrhoea therapy: A mini-review. *International Journal of Biological Macromolecules*, 122:572–577, 2019.

[29] Ranganna, S. *Handbook of analysis and quality control for fruits and vegetable products*. *Tata McGraw-Hill Education*, 1986.

[30] Reis, L. C. R. D, Facco, E. M. P., Salvador, M., Flôres, S. H. and Rios, A. de O. Antioxidant potential and physicochemical characterization of yellow, purple and orange passion fruit. *Journal of Food Science and Technology*, 55(7):2679–2691, 2018.

[31] Ren, Z. et al. Oil-in-water emulsions prepared using high-pressure homogenisation with Dioscorea opposita mucilage and food-grade polysaccharides: guar gum, xanthan gum, and pectin. *LWT - Food Science and Technology*, 162:113468, 2022.

[32] Tabilo-munizaga, G. et al. Physicochemical properties of high-pressure treated lentil protein-based nanoemulsions. *LWT-Food Science and Technology*, 101:590–598, 2019.

[33] Vega-Avila, E. and Pugsley, M. K. An overview of colorimetric assay methods used to assess survival or proliferation of mammalian cells. *Proceedings of the Western Pharmacology Society*, 54:10–14, 2011.

[34] Walia, N. and Chen, L. Pea protein based vitamin D nanoemulsions: Fabrication, stability and in vitro study using Caco-2 cells. *Food Chemistry*, 305:125475, 2020.

[35] Wang, K., Li, M., Wang, Y., Liu, Z. and Ni, Y. Effects of extraction methods on the structural characteristics and functional properties of dietary fiber extracted from kiwifruit (Actinidia deliciosa). *Food Hydrocolloids*, 110: 2021.

[36] Xu, J., Mukherjee, D. and Chang, S. K. C. Physicochemical properties and storage

stability of soybean protein nanoemulsions prepared by ultra-high pressure homogenization. *Food Chemistry*, 240:1005–1013, 2018.

[37] Yamashoji, S. and Isshiki, K. Rapid detection of cytotoxicity of food additives and contaminants by a novel cytotoxicity test, menadione-catalyzed H_2O_2 production assay. *Cytotechnology*, 37(3):171–178, 2001.

[38] Zhang, W. et al. Properties of soluble dietary fiber-polysaccharide from papaya peel obtained through alkaline or ultrasound-assisted alkaline extraction. *Carbohydrate Polymers*, 172:102–112, 2017.

[39] Zhao, S. et al. Effect of mesoscopic structure of citrus pectin on its emulsifying properties: Compactness is more important than size. *Journal of Colloid and Interface Science*, 570:80–88, 2020.

[40] Zheng, Y. et al. Effect of four modification methods on adsorption capacities and in vitro hypoglycemic properties of millet bran dietary fibre. *Food Research International*, 147:110565, 2021.